https://doi.org/10.5194/egusphere-2026-5565
Preprint. Discussion started: 25 September 2026

Temperature and Rainfall Effects on Rock Slope Dynamics: Evidence from Multi-Site Monitoring in Czechia, Central Europe

Ondřej Racek[1,2], Marco Loche[1], Filip Hartvich[1] and Jan Blahůt*[1]

1. Department of Applied Rock Mechanics, Institute of Rock Structure and Mechanics of the Czech Academy of Sciences, Prague, 18209, Czechia
2. Department of Physical Geography and Geoecology, Charles University, Prague, 128 00, Czechia

*Corresponding author: blahut@irsm.cas.cz

Abstract

Rock slopes are dynamic geomorphic systems whose stability is influenced by an interplay between geological structures and environmental forcing. Among these, meteorological variables, particularly temperature and precipitation, are recognised as key drivers of both long-term slope evolution and short to medium-term joint deformation expressed through diurnal and annual displacement cycles. However, their influence on block scale displacement remains poorly explored.

This study investigates meteorologically driven rock slope surficial dynamics using high-resolution crack meter measurements of blocks ranging in volume from 0.3 to 150 m^3 and environmental monitoring data collected from four instrumented sites in Czechia, Central Europe. Each site comprises unique geological and morphological conditions and is equipped with joint displacement sensors, a weather station, and an in-depth thermal probe. A total of twelve representative rock blocks were monitored across the sites, capturing both thermally driven and potentially gravitationally induced displacements.

We analysed multi-year time series data (≥2 years) to assess the relationships between joint movements and meteorological variables, including air temperature, in-depth rock temperature up to 3 m and rainfall. Statistical observations revealed distinct seasonal and diurnal cycles in joint dilation linked to thermal forcing. Moreover, several blocks exhibited signs of compound kinematics, with joint displacements influenced by thermal cycles, rainfall and irreversible gravitational destabilisation trends.

This study provides new insights into the temporal dynamics of rock slope instability in temperate climates. The observed thermal sensitivity highlights the importance of temperature variations in driving short-term reversible joint deformation and potentially contributing to progressive rock-slope destabilization. This study demonstrates the value of long-term, high-frequency monitoring for quantifying weather–rock mass interactions and supports the integration of kinematical interpretations into future monitoring system designs.

Keywords: thermal behaviour, rock slope stability, crack meter, joint displacement dynamics, rainfall

1 Introduction

Rock slope stability is governed by a complex interplay between internal factors, such as lithology, discontinuity geometry and rock-mass properties, and external forcing, including temperature variations, precipitation or seismic loading (Riebe et al., 2004). The evolution of the rock slope over time and its dynamics is determined by the slope's geological and morphological properties and their interactions with exogenous inputs (Morcioni et al., 2022; Rosser et al., 2007). Among the most important exogenous inputs are meteorological variables (Gariano and Guzzetti, 2016; Scaringi and Loche, 2022). The combination of slope internal properties and external factors means that every rock slope is unique and constantly changing (Pepe et al., 2014).

Rock slope dynamics includes several processes, among which rockfalls are the most hazardous (Hungr et al., 2013). Rockfall occurrence is also predisposed by the geological and morphological properties of the specific rock slope. Typically, the unstable part of the rock slope is predefined by the intersection of rock slope discontinuity systems (Priest and Hudson, 1981). Before a rockfall event occurs, often changes in joint opening can be observed. The exogenous inputs in the rock slope system affect both the rock mass and joints, thus acting as a rockfall preparatory and triggering factor (Collins and Stock, 2016; Lombardo et al., 2016).

https://doi.org/10.5194/egusphere-2026-5565
Preprint. Discussion started: 25 September 2026

Several studies have highlighted the importance of meteorological and thermal factors on rockfall activity and rock slope temporal evolution (Lombardo et al., 2014; Schneider et al., 2023). While the geological and morphological setting of a rock slope predisposes it to rockfall, meteorological variables can act as both preparatory and triggering factors (Leinauer et al., 2024), together with the effects of seismic waves propagation (Larose et al., 2015; Guillemot et al., 2022; Fei et al., 2025). The influence of meteorological factors on the rock slope stability is frequently mentioned, but still not fully understood (Scaringi and Loche, 2022). Recent monitoring in temperate environments has further shown that thermal forcing operates across multiple temporal scales, from short-term fluctuations to seasonal cycles, with its magnitude strongly dependent on local site conditions such as rock-wall orientation, shading, and fracture configuration (Gage et al., 2024). It is generally accepted that destabilisation is driven by several factors, such as thermal loading (Villarraga et al., 2018), precipitation (Sospedra-Alfonso et al., 2015), the action of ice (McCarthy et al., 2017), or rainfall (Krautblatter and Moser, 2009), among others. In high-mountain environments, thermal forcing is particularly important in relation to permafrost degradation and glacier retreat, where changes in the thermal and hydrological regime can promote both reversible thermoelastic deformation and progressive rock-slope destabilisation (Hartmeyer and Otto, 2024; Hugentobler et al., 2021).

The relationship between rock slope stability, meteorological forcing, and morphological and geological properties is complex (Araya et al., 2016). Studying the variables that influence rock slope stability requires data about all of these factors. An opportunity is to study the influence of meteorological factors on rockfall occurrence from rockfall inventories using archive data (Bajni et al., 2021). However, such datasets generally have limited temporal resolution and no information about the size of the events. To study the rock slope activity in sub-day temporal resolution, an in situ placed monitoring system is needed (Willenberg et al., 2018). The design of such a system must be site-specific to capture a particular mode of rock slope destabilisation (Elmouttie and Dean, 2020). Many examples can be found in the literature, from very simple single block monitoring systems (Collins and Stock, 2016; Lazar et al., 2018; Mulas et al., 2019) to state-of-the-art automated monitoring/warning systems, which can monitor a spatially large area (Janeras et al., 2017; Marmoni et al., 2020). A review of traditional and modern rock slope monitoring approaches is provided by Blahůt and Racek (2023) and Racek and Blahůt (2023) respectively. Rock slope dynamics, on the other hand, can be represented by various metrics, such as rockfall frequency (Hungr et al., 1999; Janeras et al., 2023), joint displacement change (Bakun-Mazor et al., 2013; Glawe et al., 1993), local seismic activity (D'Angiò et al., 2021; Liang et al., 2024) and more (Acharya and Kogure, 2022; Casagli et al., 2023). Environmental seismology provides a complementary approach, as variations in seismic properties of unstable rock slopes have been related to temperature- and rainfall-driven changes in fracture conditions and crack opening (Bottelin et al., 2024; Bottelin and Baillet, 2024). Recent long-term monitoring has further demonstrated that repeated natural thermal cycles produce predominantly reversible thermoelastic joint deformation over short timescales, while progressive displacement may develop over multi-year periods, indicating a potential cumulative effect of thermal cycling on rock-slope evolution (Gasc-Barbier et al., 2024). When both rock slope dynamics and meteorological variables are monitored, the resulting time series statistical model that describes rock slope dynamics in relationship with exogenous variables can be constructed (D'Amato et al., 2016; Macciotta, 2019). Furthermore, crack meter data can be used for rock slope numerical model calibration and future prediction (Pasten et al., 2015; Racek et al., 2025). Indeed, monitoring may reveal accelerating displacement associated with progressive destabilisation and an increasing likelihood of failure, although the exact timing of collapse generally remains highly uncertain (Marjanovic et al., 2021; Zvelebill and Moser, 2001).

As highlighted from the literature reviewed above, thermal forcing and other weather-related variables play an important role in the rock slope evolution. However, most existing studies are based on single-site observations or focus on monitoring of individual rock slope features. As a result, the possibility of identifying general relationships between rock slope dynamics and exogenous forcing remains limited. Broader multi-site studies across different geological and morphological settings are still largely missing.

In this study, we analyse high-frequency crack meter data from four instrumented rock slopes in Czechia. These sites represent different lithologies, slope morphologies, aspects, and climatic regimes. By integrating crack meter monitoring with in-depth rock mass temperature measurements and meteorological observations, we investigate how these variables influence the dynamics of various partial rock blocks.

The originality of this work lies in the comparative multi-site approach. The variety of environments and block dynamic regimes allows us to use a large dataset to identify how different block configurations respond to thermal and meteorological forcing. Our results show that the geometry and kinematics of monitored rock slope features

https://doi.org/10.5194/egusphere-2026-5565
Preprint. Discussion started: 25 September 2026

exert stronger control on joint displacement dynamics than lithology or local climatic regime, highlighting the importance of careful monitoring system design.

2 Materials and Methods

2.1 Study sites and instrumentation

We used data collected using similar monitoring instrumentation at four rock slopes in Czechia, Central Europe over a period 2018–2024 (**Fig. 1a**). In this section, we introduce four monitored rock slopes in Czechia, Central Europe, together with their geological and geomorphological settings. The sites were selected to represent contrasting geological, morphological, and local climatic conditions, while their basic characteristics and thermal regimes together with monitoring period are summarized in Table 1. Occasional gaps in the time series occurred due to temporary sensor malfunction or battery discharge and were retained as missing data without interpolation. Pastýřská Rock is a blocky sandstone rock slope characterized by mutually perpendicular discontinuity sets, whereas Branická Rock is formed by Devonian limestones with bedding-controlled block geometries. Tašovice represents a highly fractured and weathered granitic rock slope with several potentially unstable blocks, while Labský důl is a high-elevation granitic rock slope characterized by a colder mountain climate and structurally controlled rockfall activity. Detailed descriptions of the individual sites and monitored rock-slope features are provided in Sections 2.1.1–2.1.4.

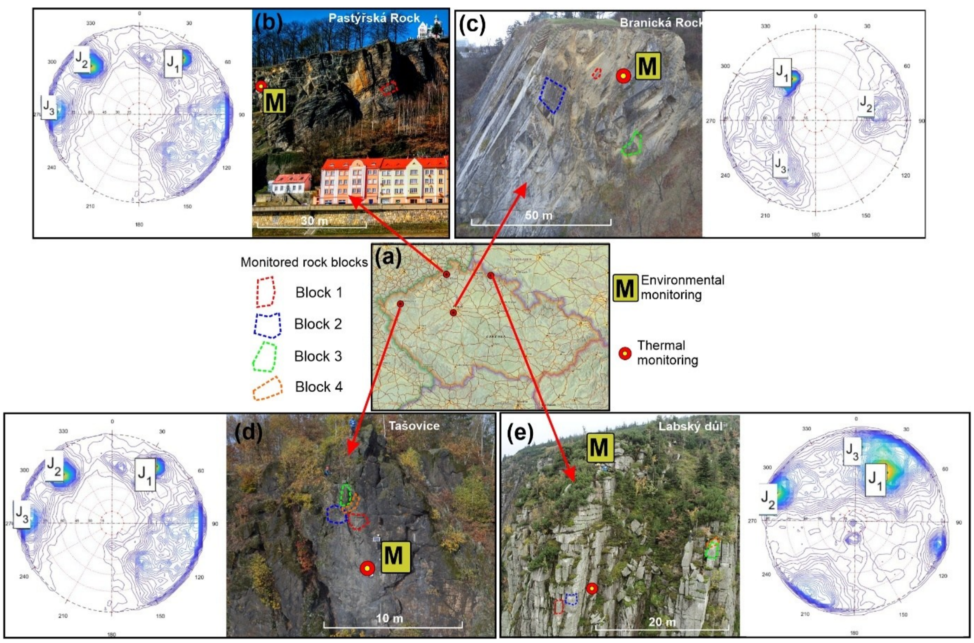

Figure 1. Location of the four monitoring sites in Czechia: (a) Overview of the monitoring sites; monitored blocks are highlighted by dashed lines in different colours, together with the locations of environmental and thermal monitoring within the rock slopes. Basemap: Esri National Geographic Style Map. (b) Detail of the Pastýřská Rock site; (c) overview of the Branická Rock site; (d) overview of the Tašovice monitoring site; (e) overview of the Labský důl site. Pole-density plots represent the main discontinuity sets at each monitored site.

Table 1. Description of the sites. Coordinates of rock slopes, aspect, rock type and basic thermal regime at all sites.

Site	Pastýřská Rock	Branická Rock	Tašovice	Labský důl
Coordinates [lat/lon]	50.7797606N / 14.2048478E	50.0408292N / 14.4119519E	50.2112244N / 12.8085594E	50.7589736N / 15.5473631E
Altitude [m.a.s.l.]	220	250	410	1300
Aspect	NE	NW	SE	N
Rock type	Sandstone	Limestone	Granite	Granite
Average T [°C]	12.49	12.69	9.22	4.59
surface temperature span [°C]	-2.28–41.38	-5.02–48.36	-4.97–46.68	-9.46–33.66
No. of freeze–thaw cycles per year	16	22	32	97
Monitoring period	X.18–VIII.25	V.19–VIII.25	XI.20–VIII.25	XII.18–VIII.25

These rock slopes are instrumented with a modular monitoring system consisting of three components:

- **Joint dilatation monitoring** is carried out on selected joints that define partial rock blocks. For this, induction crack meters with a measurement range of 200 mm, resolution of 0.05 mm, repeatability of 0.01 mm, and accuracy better than 0.1% are used. With this instrumentation, we can capture both thermally driven joint opening/closure and possible trends represented by irreversible joint behaviour. The monitoring frequency is one hour. The characteristics of the monitored joints and crack-meter installations are summarized in Table 2.
- **Environmental monitoring** of meteorological variables is performed by an automated weather station placed directly on the rock slopes ensuring that the recorded meteorological conditions are representative of the monitored site. To get information about the influence of meteorological variables, weather station monitoring should be placed as close to the monitored slope as possible (Macciotta et al., 2015; Matsuoka, 2019). A weather station monitors air temperature, precipitation, atmospheric pressure, air humidity, and incoming/reflected solar radiation. Monitoring frequency is ten minutes.
- **Thermal monitoring** is provided by a custom in-depth temperature probe placed in a 3 m deep horizontal borehole. The thermocouples are placed on the rock surface and at depths of 0.05, 0.1, 0.2, 0.3, 0.5, 1.0, 1.5, 2.0, 2.5 and 3.0 m. With this instrumentation, we are able to observe short- (diurnal) and long-term (annual) temperature cycles in the shallow rock slope surficial zone with a monitoring frequency of 10 minutes.

https://doi.org/10.5194/egusphere-2026-5565
Preprint. Discussion started: 25 September 2026

Table 2. Characteristics of monitored block, joints and crack-meter installation. The angle to joint represents the angle between the crack-meter axis and the joint plane; 90° indicates perpendicular installation.

Site	Block	Block dimensions [m]	Crack meter	Joint aperture [mm]	Mean CM position [mm]	Angle to joint [°]
PAS	P1	6.7 × 10.7 × 2.5	PS1_1	250	100.19	45
			PS1_2	210	57.12	90
			PS2_1	25	197.4	90
			PS2_2	50	99.04	90
BRA	B1	0.8 × 1.4 × 0.4	BRA1_1	150	53.6	90
			BRA1_2	150	73.13	60
	B2	0.9 × 4.5 × 3.7	BRA2_1	25	109.09	90
			BRA2_2	35	131.03	90
			BRA4_1	350	108.04	45
	B3	2.5 × 1.6 × 3.6	BRA3_1	10	80.78	90
			BRA3_2	10	21.47	10
TAS	T1	1.7 × 1 × 2.1	TAS1_1	160	62.74	80
	T2	0.9 × 0.8 × 0.4	TAS2_1	10	130.52	90
			TAS2_2	15	124.54	90
	T3	0.5 × 1.2 × 0.4	TAS3_1	250	116.26	90
			TAS3_2	150	112.12	90
	T4	1 × 1.5 × 0.8	TAS1_2	180	90.55	90
LAB	L1	1.4 × 0.7 × 0.35	LAB1_1	160	3.06	90
	L2	0.9 × 1.1 × 0.5	LAB1_2	140	114.01	90
	L3	0.6 × 1 × 0.7	LAB3_1	200	89.34	80
	L4	1.35 × 1.8 × 0.65	LAB3_2	10	123.21	10

Thermal monitoring enabled the definition of surficial zone thermal metrics. From in-depth temperature data, the theoretical stable temperature depth (STD) and long-term stable temperature (LST) of the rock can be calculated. LST is determined by long-term air temperature at the site, whereas STD is defined as a depth of the rock where annual variations do not exceed 0.1 °C.

Across four sites, a total of twelve rock blocks is instrumented with twenty-one crack meters. Based on their structural setting, the blocks can be categorized according to their anticipated temporal dynamics. Two blocks are classified as long-term stable, secured within the rock slope (P1, T1), with measured displacements expected to reflect only thermally driven expansion and contraction. Three blocks are arranged in a configuration prone to toppling instability (B1, T3, L1). Four blocks (B2, B3, T2, L2) are expected to slide along their basal surfaces, whereas three blocks are positioned in a wedge/ratchet setting (L3, L4, T4). This block classification represents the destabilization mechanism identified during the monitoring design phase. All monitored blocks are affected by meteorological forcing, such as rainfall, wind, and water phase changes, thus the overall destabilization patterns are complex.

2.1.1 Pastýřská Rock

The first monitoring site is Pastýřská Rock. The studied rock slope is situated in northern Bohemia on the left bank of the Labe River, within the town of Děčín (**Fig. 1a**), at an altitude of 220 m above sea level. The rock slope has a long history of rockfall activity, with larger rockfalls involving several cubic metres of material occurring

https://doi.org/10.5194/egusphere-2026-5565
Preprint. Discussion started: 25 September 2026

approximately once every 10–20 years during the first half of the 20th century. Small-scale rockfalls occur continuously, with increased activity particularly during spring and rainfall events. Mitigation measures were therefore implemented during the 1980s using anchoring of unstable blocks. The rock slope is over 50 m high, and it is formed by Cretaceous sandstone, with variable properties (**Table 1**). The nearly vertical rock wall, including overhanging sections, is oriented towards the SE. Three main discontinuity sets (**Fig. 1b**) (dip/dipdir: 80°/40°, 86°/310°, 80°/275°) cut the rock slope into semi-rectangular blocks.

From a geomorphological point of view, Pastýřská Rock is a typical representative of sandstone cuesta (Vařilová et al., 2022). The rock slope was formed by increased river erosion at the end of the Pleistocene. During this period, the Labe River, which originally flowed around the cuesta from the west, incised through and formed a water-gap valley. Pastýřská Rock is a steep bank of this valley. Subsequently, the rock slope was exposed to fluvial erosion as part of the outer cut bank. The increased fluvial erosion led to the destabilization and increase in the slope, inclination, and even the formation of overhanging parts of the rock slope (Engel and Kalvoda, 2001; Vařilová et al., 2022).

Rock block monitoring with crack meters was established in 2018 and has since provided data at 1 h temporal resolution. At this site, one large block (P1) with dimensions 6.7 × 10.7 × 2.5 m is monitored, using four crack meters (**Fig. 2**). This monitored rock block was not anchored during the past mitigations, so we can expect its behaviour to be naturally driven. Although this block is relatively large and wedged within the rock slope, there is no expectation of sudden destabilisation. The four crack meters (PS1_1, PS1_2, PS2_1, PS2_2) are arranged to monitor thermally driven expansion and dilatation of the block in four directions (**Fig. 2**). The weather station, together with the compound borehole thermal probe, is located directly within the rock slope (**Fig. 1b**).

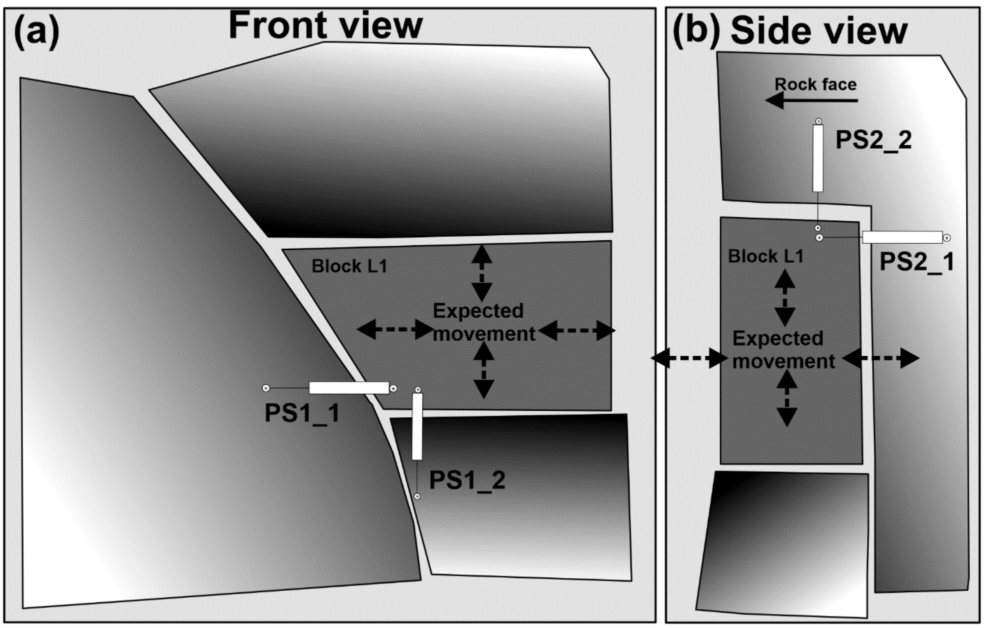

Figure 2. Schematic presentation of the crack meter monitoring within the Pastýřská stěna site. Crack meter placement in relation with monitored block with expected movement is presented using front view **(a)** and side view **(b)**. Rock face direction is marked by a solid pointer, and expected block movement is marked by dashed pointers. Grey background indicates rock mass behind monitored blocks.

2.1.2 Branická Rock

This rock slope in Prague central Czechia (**Fig. 1c**) was instrumented in the summer of 2019. The rock slope is formed by Devonian limestone layers and was artificially created by quarrying (including blasting), which was carried out on the site until the 1930s. The studied rock slope is situated on the right bank of the Vltava River and

https://doi.org/10.5194/egusphere-2026-5565
Preprint. Discussion started: 25 September 2026

has a general WSW-facing orientation, at an elevation of 250 m above sea level. The weather station is placed on a rock slab dipping 80° to the SW (235°). Three main discontinuity sets (dip/dip dir: 50°/325°, 64°/81°, and 62°/210°) were identified (**Fig. 1c**); these represent the limestone layers and the rock face created by quarrying.

The rock slope was initially created by river erosion of the Vltava River through the anticlinal structure of the eastern part of Barrandien, which continues to the southwest on the left Vltava riverbank. These erosional processes were active mainly during the Pleistocene, when the evolution of the rock slope took place in the last glacial period. The current morphology of the rock slope is caused by limestone quarrying. The current shape is the result of intensive mining operations, including blasting, which formed a rockfall-susceptible and often overhanging rock face. This setting has resulted in recurrent rockfall activity, including a major event in 1874 and continued activity after quarry closure. Small-scale rockfalls occur frequently (every year), particularly following freeze–thaw cycles and intense rainfall, while larger detachments of up to approximately 1–2 m^3 occur at intervals of several years. Mitigation measures included removal of unstable material, anchoring of unstable blocks, and installation of protective nets and steel barriers to reduce rockfall hazard below the slope.

Three unanchored blocks (**Fig. 3**) are monitored using a total of seven crack meters at this site. Three blocks (B1–B3) are monitored at Branická Rock. Block B1 is the smallest monitored block (0.8 × 1.4 × 0.4 m) and is located in a highly weathered part of the rock slope. It is monitored by two crack meters (BRA1_1 and BRA1_2) oriented in the direction of expected toppling destabilisation (**Fig. 3a**). Block B2, located in the upper part of the rock slope, is the largest monitored block (0.9 × 4.5 × 3.7 m) and consists of a 1.6-m-thick limestone layer. The block is expected to slide along the underlying surface, and its movement is monitored by three crack meters (BRA2_1, BRA2_2 and BRA4_1) (**Fig. 3c, d**). Block B3 is located at the bottom of the rock slope, partly shaded by vegetation, and has dimensions of 2.5 × 1.6 × 3.6 m. It lies between limestone layers and is expected to undergo sliding, which is monitored by two crack meters (BRA3_1 and BRA3_2) (**Fig. 3e**). The weather station and thermal probe are located in the upper part of the rock slope.

https://doi.org/10.5194/egusphere-2026-5565
Preprint. Discussion started: 25 September 2026

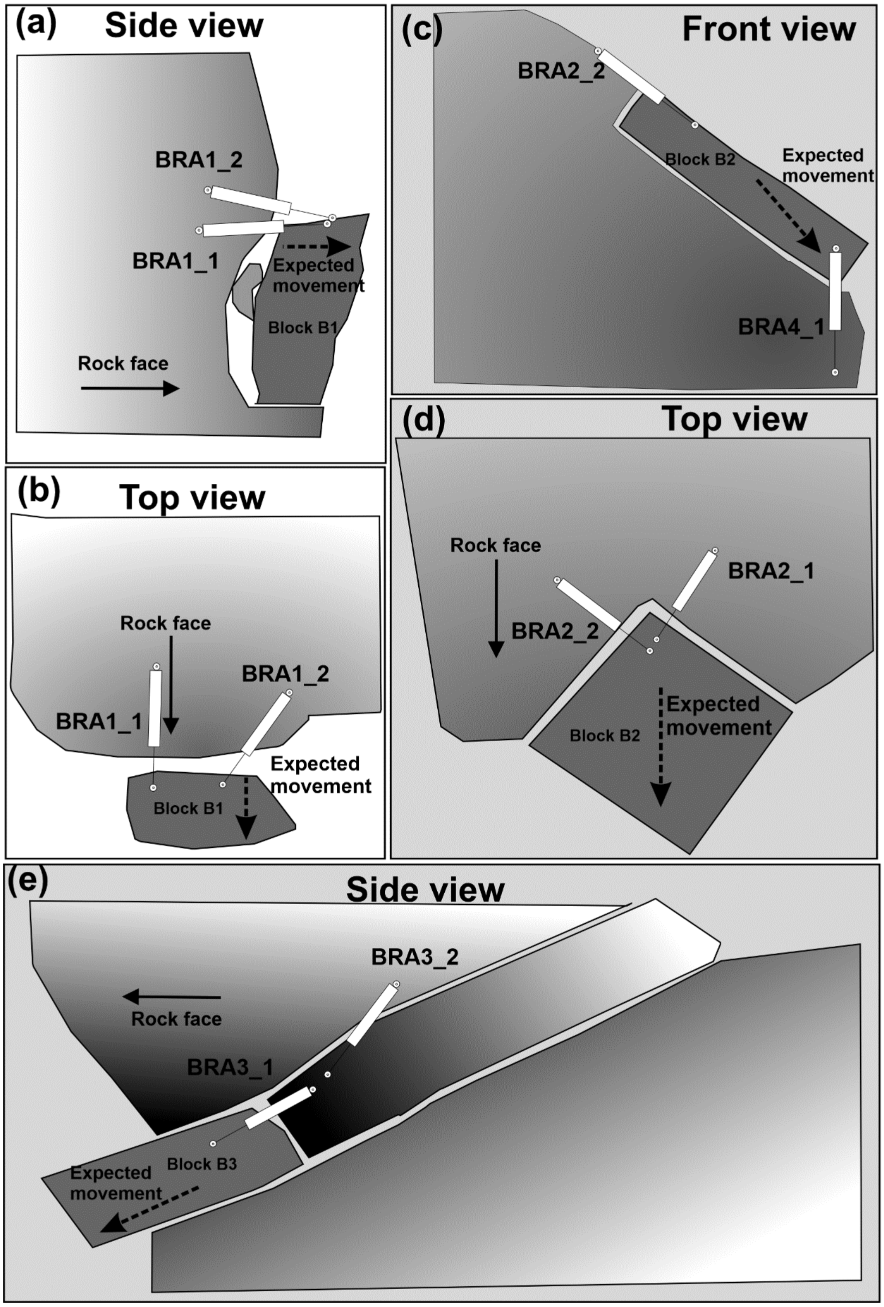

Figure 3. Schematic sketch of 3 monitored rock blocks within the Branická rock site. Block 1 side view **(a)** and top view **(b)**, block 2 side view **(c)** and top view **(d)**, block 3 side view **(e)**. Rock face direction is marked by solid pointers, and expected block movements are marked by dashed pointers. Grey background indicates rock mass behind monitored blocks.

https://doi.org/10.5194/egusphere-2026-5565
Preprint. Discussion started: 25 September 2026

2.1.3 Tašovice

The third instrumented site is a rock slope (**Fig. 1d**) located above a local road on the left bank of the Ohře River, in western Czechia (**Fig. 1a**). The rock slope is formed by granite with varying degrees of weathering. It faces SSE and reaches an altitude of 410 m a.s.l. The slab where the weather station with the borehole probe is placed is dipping 88° to the south. Three relatively poorly developed discontinuity sets (dip/dipdir: 50°/85°, 50°/320°, 88°/272°) were identified (**Fig. 1d**). At this site, small rockfalls, typically involving fragments with dimensions of up to approximately 10 cm, occur frequently. Based on observations of fresh debris accumulations below the rock face, particularly following major rainfall events, their recurrence is estimated to range from several days to several months.

Both the rock slope and the associated river valley are structurally controlled by a tectonic fault, which is reflected in the rock face aspect. The evolution of the steep slope is controlled by fluvial erosion, owing to its position on the outer bank of the river meander. Four relatively small blocks are monitored at this site (**Fig. 4**). Block T1 (1.7 × 1 × 2.1 m), Block T2 (0.9 × 0.8 × 0.4 m), Block T3 (0.5 × 1.2 × 0.4 m), and Block T4 (1 × 1.5 × 0.8m). The largest block at this site (T1) is monitored by one crack meter, TAS1_1. The measurement setup is designed to capture the thermal expansion and contraction of the partial block. Nevertheless, the crack meter TAS1_1 simultaneously reflects the dynamics of block T2, potentially affecting the recorded temporal displacement. Block T2 is monitored by two crack meters: one is placed vertically (TAS2_1), the second one, TAS2_2, is placed horizontally, measuring possible destabilization in the rock face direction. The dynamic of the block T2 is expected to be a combination of gravitationally driven destabilisation and thermally induced volumetric changes, with possible influence of the wedge (block T4). In the case of the block T3, a toppling movement is expected and monitored by two crack meters. The first one (TAS3_1) is monitoring the expected upper joint opening, while the second one is monitoring consequential lower joint closure (TAS3_2). Block T4, where we expect a combination of gravitational wedging combined with thermally induced volumetric changes, is monitored by one crack meter (TAS1_2).

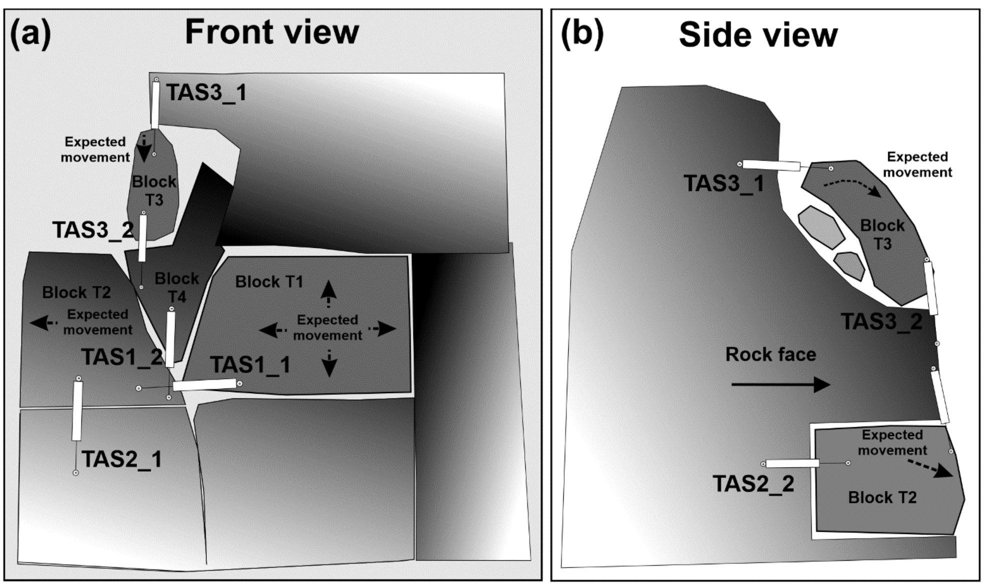

Figure 4. Schematic sketch of four monitored rock blocks within Tašovice site. Front view of all monitored blocks **(a)** and side view of blocks 2 and 3 **(b)**. Rock face direction is marked by solid pointers, expected block movements are marked by dashed pointers. Grey background indicates rock mass behind monitored blocks.

https://doi.org/10.5194/egusphere-2026-5565
Preprint. Discussion started: 25 September 2026

2.1.4 Labský důl

The last monitoring site, established in 2020, is Labský důl. The site is located in the Krkonoše mountains (**Fig. 1a**) at an altitude of 1300 m a.s.l. on the edge of a glacially shaped valley (**Fig. 1e**). The rock slope is formed by granite and faces north. The weather station is located at the upper edge of the rock slope, and the temperature probe is placed within the slab facing NW. In the field, four discontinuity sets (dip/dipdir: 67°/32°, 86°/290°, 80°/5°, 24°/198°) were identified (**Fig. 1e**). Geodynamic processes remain highly active in this area due to the young glacially formed relief. Small-scale rockfalls (<1 m³) occur regularly, with the highest activity during spring snowmelt in April and May, as indicated by field observations during monitoring inspections and by Krause and Pilous (2020). Larger rockfalls (>1 m³) are less frequent, with estimated recurrence intervals of 10–30 years, typically associated with intense rainfall or rapid snowmelt. Large Holocene rock-slope failures (>1,000 m³) have also been documented, although no such event has occurred in modern history (Krause and Pilous, 2020).

The valley of Labský důl was carved by glaciers during the late Pleistocene, when the thickness of the glacier was estimated at over 200 m. After deglaciation, the slopes became naturally unstable as they lost glacial ice support (Engel et al., 2010; Krause, 2021). The rock slope is located directly on the edge of the cirque, where the altitude difference between the cirque floor and mountain plateau is over 300 m. The valley was glacially overdeepened by more than 150 m. Following deglaciation, the rock slope became exposed to severe subalpine conditions associated with its northern orientation. Repeated freeze–thaw cycles, reaching up to 97 cycles per year, contribute to the destabilization of partially detached blocks and increase overall rockfall susceptibility. During winter, the upper parts of the slope are also characterized by substantial snow accumulation, including the formation of snowdrifts and local ice accumulation.

On this site, four blocks are monitored using 4 crack meters (**Fig. 5**). Block L1 (1.4 × 0.7 × 0.35 m) is located within the rock face, and the crack meter LAB1_1 monitors the expected toppling destabilisation. Block L2 (0.9 × 1.1 × 0.5 m) lies freely within the rock face; its destabilisation is monitored by crack meter LAB1_2. Block L3 (0.6 × 1 × 0.7 m) forms a wedge between stable rock and block L4 (1.35 × 1.8 × 0.65 m). The wedging/ratcheting setting formed by these two blocks is monitored by two crack meters, LAB3_1 (wedge) and LAB3_2 (wedged block). Block L3 is expected to act as a wedge, pushing block L4 in the rock face direction. In the case of the wedge block, we expect the closing of the crack meter, whereas in the case of block L4, the crack meter should be gradually elongated when the block is pushed by the wedge in the rock face direction.

https://doi.org/10.5194/egusphere-2026-5565
Preprint. Discussion started: 25 September 2026

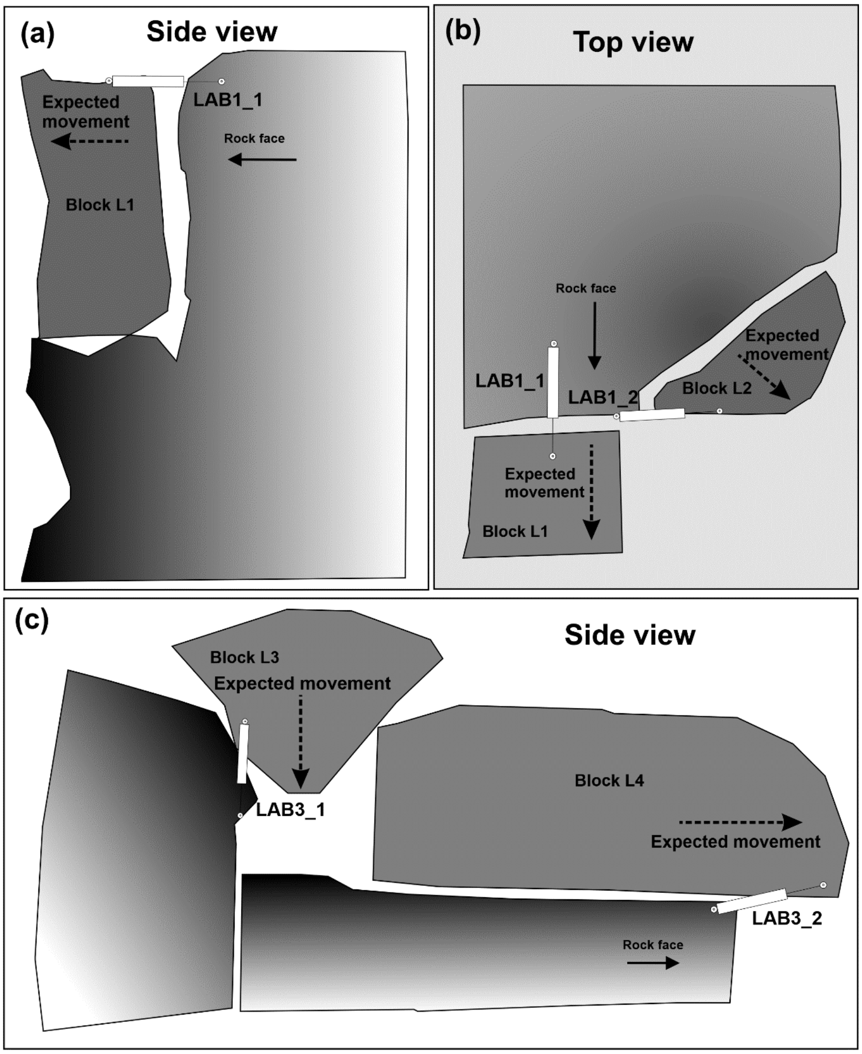

Figure 5. Schematic presentation of the monitored partial blocks within the Labský důl site. **(a)** Block L1 side view. **(b)** Blocks L1 and L2 top views. **(c)** Blocks L3 and L4 side view. Rock face direction is marked by solid pointers and expected block movements are marked by dashed pointers. Grey background indicates rock mass behind monitored blocks.

2.2 Methods

Blocks and crack meters were categorised according to their expected failure modes (e.g., toppling, sliding, wedging/ratcheting) and by local structural settings. This methodological framework enabled comparative analysis across different lithologies, structures, and block configurations, yielding insight into the mechanistic links between external meteorological forcing and response of the rock slope surficial zone formed by partial blocks.

2.2.1 Influence of temperature

Data processing focused mainly on identifying the influence of temperature and rainfall on crack meter positions. The main aim was to identify thermally and rainfall-driven joint opening and closure dynamics. To do this, we analysed hourly time series of crack meter positions together with environmental monitoring data, which are air temperature (weather station), air temperature measured by crack-meter datalogger, rock mass surface temperature, and rock temperature at depths of 150 and 300 cm and hourly rainfall totals. To investigate the relationship between the above-mentioned variables and rock slope dynamics, we employed a data-driven approach, where we analysed a minimum of two years of continuous data per site (max 5 years), allowing seasonal and interannual variability to be captured. Time series were processed to evaluate thermally driven components using correlation analysis with surface and subsurface temperatures, while descriptive statistics were applied to identify and quantify the influence of environmental variables on crack meter dynamics. Furthermore, for all deployed crack meters average annual and diurnal displacement amplitudes and irreversible displacement trends in mm/year were calculated. This allowed us to explore kinematic modes of all deployed crack meters.

2.2.2 Influence of rainfall

For rainfall influence, we additionally explored longer-lasting precipitation periods, not only correlations with measured rainfall intensity in mm/h. Rainfall and temperature show covariation at different temporal scales: seasonally, most precipitation occurs during the warmer part of the year, while individual rainfall events are often accompanied by rapid decreases in air and rock-surface temperature. As a first step, both annual and diurnal seasonality were removed from the displacement data using multi-seasonal STL (Bandara et al., 2025; Cleveland et al., 1990), to obtain seasonally adjusted displacement residuals. Afterwards, the rainfall effect was analysed using event-based analysis of position-residual responses (Nava et al., 2024). This analysis was used to uncover rainfall-related responses that could not be captured by direct correlation analysis, particularly delayed and cumulative responses following precipitation events. The data were processed in R, similarly to what was proposed by Leinauer et al. (2024). Descriptive statistics helped in summarising and presenting the main features of the large time series quantitatively, providing a clear overview.

To evaluate the influence of extreme precipitation on residual crack-meter deformation, we applied an event-based, non-parametric response analysis. This approach was adopted to identify delayed and cumulative crack-meter responses following rainfall events that may not be captured by direct correlations with hourly rainfall totals. Extreme precipitation events were defined using a quantile-based threshold (Q90) of rolling precipitation sums calculated over multiple accumulation windows (24–96 h). For each event, cumulative residual displacement was evaluated within fixed post-event response windows (72–240 h). Namely, the combinations of Q90 rainfall extremes and response windows were:

- **24 h/72 h**: rainfall event Q90 24 h, with response window 72 h
- **24 h/168 h**: rainfall event Q90 24 h, with response window 168 h
- **24 h/240 h**: rainfall event Q90 24 h, with response window 240 h
- **48 h/72 h**: rainfall event Q90 48 h, with response window 72 h
- **48 h/168 h**: rainfall event Q90 48 h, with response window 168 h
- **48 h/240 h**: rainfall event Q90 48 h, with response window 240 h
- **72 h/168 h**: rainfall event Q90 72 h, with response window 168 h
- **72 h/240 h**: rainfall event Q90 72 h, with response window 240 h
- **96 h/168 h**: rainfall event Q90 96 h, with response window 168 h
- **96 h/240 h**: rainfall event Q90 96 h, with response window 240 h

The distribution of post-event responses was compared against a control (placebo) distribution sampled from non-event periods using the Mann–Whitney U test (MacFarland and Yates, 2016). This approach allows detection of delayed and cumulative deformation responses while remaining robust to non-Gaussian residual noise. Using this approach, statistically significant effects of rainfall events on crack meter displacement residuals were identified for different rainfall-event and response-window combinations.

2.2.3 Cluster analyses

The final analytical step involved hierarchical, process-oriented clustering of crack meters based on dominant environmental forcing (**Fig. 6**). The objective was to group the crack meters into clusters representing physically interpretable deformation mechanisms. Both temperature and rainfall relationships were analysed for all crack meters. The hierarchical structure applies only to their subsequent classification: crack meters showing a dominant

https://doi.org/10.5194/egusphere-2026-5565
Preprint. Discussion started: 25 September 2026

relationship with temperature were classified first, whereas rainfall-event responses were subsequently used to classify those not assigned to the temperature-driven groups. In the first step, temperature-driven crack meters were identified using the Pearson correlation coefficient between absolute crack displacement and temperature measured by the data logger. Absolute values rather than derivatives or seasonally adjusted data were used because the analysis aimed to identify the dominant temperature-related cyclic response, including its seasonal component. Crack meters with an absolute correlation coefficient exceeding 0.4 were classified as temperature-driven. This temperature-controlled group was further subdivided into two clusters: Cluster 1 (CL1) consisted of crack meters exhibiting negative correlations with temperature, whereas Cluster 2 (CL2) comprised crack meters with positive temperature correlations. The remaining crack meters were subsequently classified based on the results of rainfall event-response analysis of seasonally adjusted displacement residuals. Cluster 3 (CL3) includes crack meters showing a statistically significant response to extreme rainfall events in more than one event/response combination. Finally, Cluster 4 (CL4) consists of crack meters exhibiting complex behaviour, with no statistically significant relationship to either temperature or rainfall forcing.

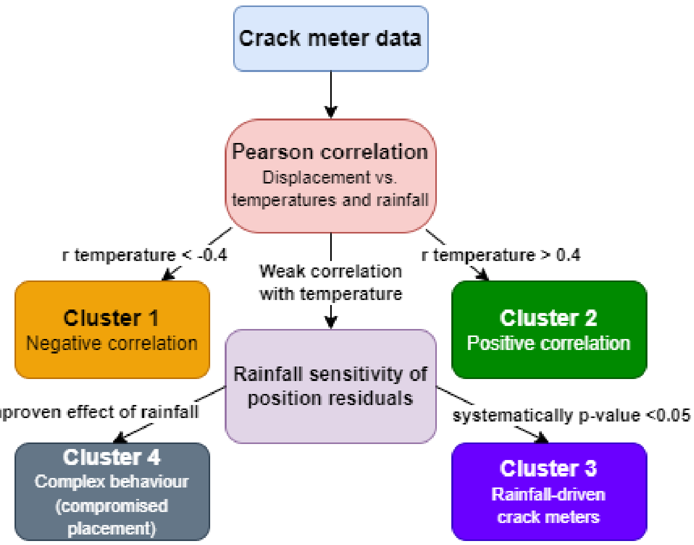

Figure 6. Hierarchical clustering based on thermal and rainfall response of crack meters.

Finally, the interrelationships among block failure mode, crack meter configuration, and external deformation drivers were investigated to establish more generally applicable insights into the response of different destabilization mechanisms to external forcings. From this analysis, we were able to define general patterns for how crack meters monitoring different rock slope features respond to temperature and rainfall forcing.

https://doi.org/10.5194/egusphere-2026-5565
Preprint. Discussion started: 25 September 2026

3 Results

The results are presented at both site-specific and cross-site levels. First, the thermal regime and crack-meter displacement characteristics, including responses to extreme rainfall events, are described separately for each monitoring site. Subsequently, temperature- and rainfall-related displacement dynamics are evaluated across the complete dataset. Finally, hierarchical clustering is used to identify groups of crack meters with similar responses to the monitored environmental variables.

3.1 Site specific thermal and displacement characteristics

The thermal regime and crack-meter displacement characteristics were evaluated separately for each monitoring site. The site-specific results include thermal conditions, diurnal and annual crack-meter displacement patterns, long-term displacement trends, and relationships between crack-meter position and temperature. In addition, the response of crack-meter displacement residuals to extreme rainfall events was evaluated at each site to identify statistically significant rainfall-related responses. The long-term thermal characteristics, including stable temperature depth (STD), long-term stable temperature (LST), and the attenuation of daily temperature amplitudes with depth, are displayed in **Fig. 7**. These averages were calculated from all data within monitoring periods presented in Table 1.

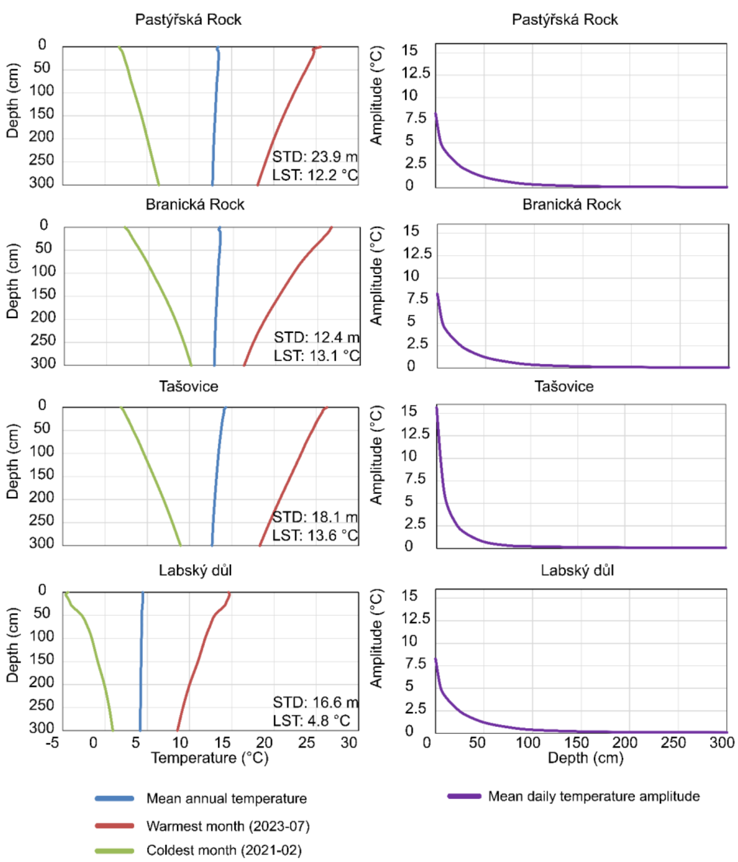

Figure 7. Basic long-term variables of the monitored rock slopes. On the left are rock temperature profiles from the surface to 3 m depth showing mean annual temperature, temperature of the coldest and warmest month within the period of 12/2020–11/2023, and calculated STD and LST. On the right side, mean daily temperature amplitudes on the different sites are shown.

https://doi.org/10.5194/egusphere-2026-5565
Preprint. Discussion started: 25 September 2026

3.1.1 Pastýřská Rock

Pastýřská Rock reaches a mean annual temperature of 12.49 °C, with a long-term stable temperature (LST) of 12.2 °C and stable temperature depth (STD) of 23.9 m. The site exhibits lower daily temperature amplitudes in the near-surface zone compared with Branická Rock and Tašovice. Daily temperature amplitudes decrease exponentially with depth and are observable to approximately 75 cm during the warm period and 50 cm during the cold period.

The Pastýřská Rock site consists of one large block (P1) monitored by four crack meters. The data show a strong and consistent diurnal signal in joint aperture, closely coupled with the measured temperatures (**Table 3; Fig. 8**). All deployed crack meters show both diurnal and annual displacement amplitudes. The measured displacement pattern is largely reversible: during colder periods, the crack meters elongate, whereas during warmer periods they contract. Relatively high annual and diurnal amplitudes are observed, while all four sensors show slight long-term closing trends (**Table 3**). The relationship between crack-meter position and temperature is consistent across all sensors, with negative linear regression coefficients ranging from −0.012 to −0.0199 mm/°C.

https://doi.org/10.5194/egusphere-2026-5565
Preprint. Discussion started: 25 September 2026

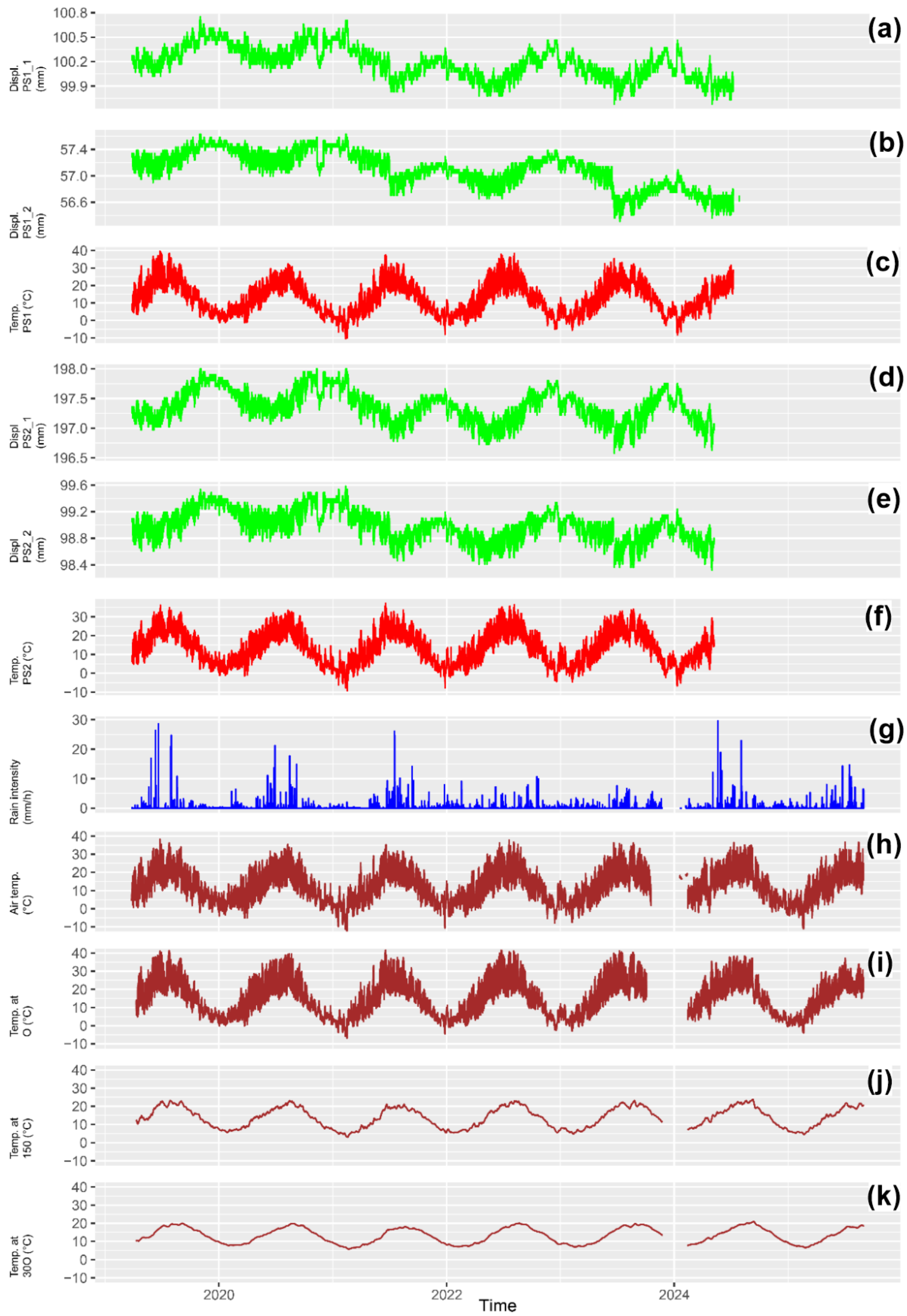

Figure 8. Analysed data from Pastýřská Rock between 2020 and 2024, aggregated to 1 h resolution. **(a)** Displacement PS1_1 (mm); **(b)** Displacement PS1_2 (mm); **(c)** temperature PS1 (°C); **(d)** Displacement PS2_1 (mm); **(e)** Displacement PS2_2 (mm); **(f)** temperature PS1 (°C); **(g)** rainfall intensity (mm/h); **(h)** air temperature weather station; **(i)** rock slope surface temperature; **(j)** temperature 150 cm; **(k)** temperature 300 cm.

Statistically significant rainfall-related responses were detected for PAS1_2 and PAS2_2, each for only one rainfall/response-window combination (Table 4). No significant responses were detected for PAS1_1 and PAS2_1. Thus, no systematic rainfall response was observed at Pastýřská Rock.

3.1.2 Branická Rock

Branická Rock is the warmest monitored site, with an average annual temperature of 12.69 °C. The long-term stable temperature (LST) reaches 13.1 °C, while the stable temperature depth (STD) is 12.4 m. The site shows relatively high daily temperature amplitudes in the near-surface zone, which decrease exponentially with depth.

Branická Rock shows variable crack-meter displacement patterns across the three monitored blocks (B1–B3) (**Table 3; Fig. 9**). Block B1, monitored by two crack meters (BRA1_1 and BRA1_2), shows diurnal and seasonal displacement signals superimposed on progressive opening of both crack meters, with an acceleration during the winter period of 2023/2024. The linear regression coefficients between crack-meter position and temperature are low, while the progressive opening is more pronounced for BRA1_1. Block B2 is monitored by three crack meters (BRA2_1, BRA2_2 and BRA4_1), which show relatively stable and reversible displacement patterns. Both annual and diurnal amplitudes are present, with the highest diurnal amplitudes measured during the spring season, while the linear regression coefficients with temperature are low. No significant joint-opening trend is observed for BRA2_1 and BRA2_2, whereas BRA4_1 shows a slow closing trend. Block B3, monitored by BRA3_1 and BRA3_2, shows highly variable displacement, with both crack meters exhibiting similar patterns, low negative long-term trends, and a relatively low but measurable relationship with temperature. The highest diurnal amplitudes for both crack meters were measured in October.

https://doi.org/10.5194/egusphere-2026-5565
Preprint. Discussion started: 25 September 2026

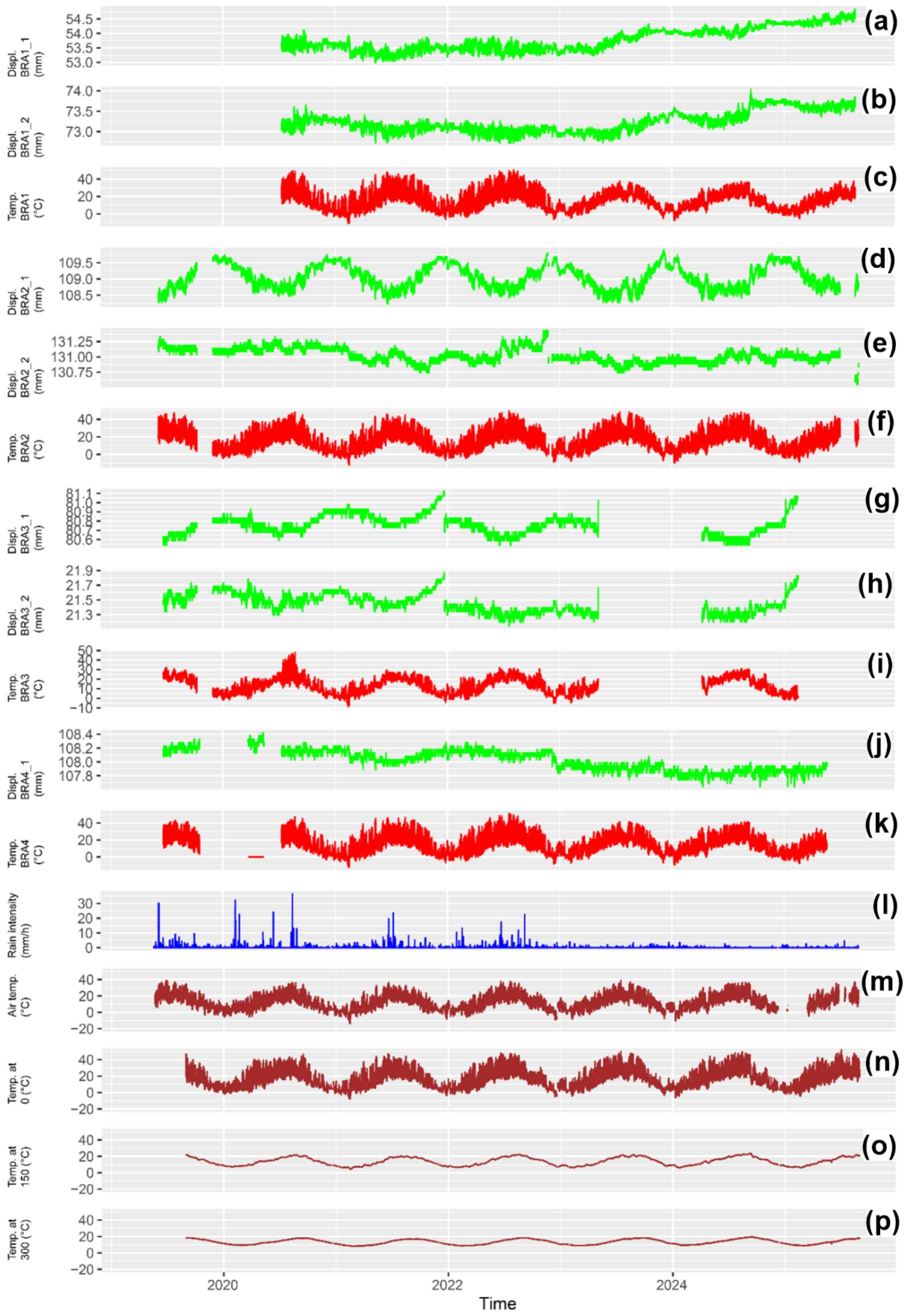

Figure 9. Analysed data from Branická Rock between 2020 and 2023, aggregated to 1 h resolution. **(a)** Displacement BRA1_1 (mm); **(b)** Displacement BRA1_2 (mm); **(c)** temperature BRA1 (°C); **(d)** Displacement BRA2_1 (mm); **(e)** Displacement BRA2_2 (mm); **(f)** temperature BRA2 (°C); **(g)** Displacement BRA3_1 (mm); **(h)** Displacement BRA3_2 (mm); **(i)** temperature BRA_3; **(j)** Displacement BRA4_1 (mm); **(k)** temperature BRA4; **(l)** rainfall intensity (mm/h); **(m)** air temperature weather station; **(n)** rock slope surface temperature; **(o)** temperature 150 cm; **(p)** temperature 300 cm.

https://doi.org/10.5194/egusphere-2026-5565
Preprint. Discussion started: 25 September 2026

Statistically significant rainfall-related responses were detected for BRA1_1, BRA1_2, and BRA2_2 (Table 4). BRA2_2 showed significant responses for five rainfall/response-window combinations and BRA1_1 for three combinations, whereas BRA1_2 showed a significant response for only one combination. No significant responses were detected for the remaining crack meters.

3.1.3 Tašovice

Tašovice Rock has an average annual temperature of 9.22 °C. The long-term stable temperature (LST) reaches 13.6 °C, while the stable temperature depth (STD) is 18.1 m. Relatively high daily temperature amplitudes are observed in the near-surface zone and decrease exponentially with depth.

Tašovice Rock shows variable crack-meter displacement patterns across the four monitored blocks (T1–T4) (**Table 3; Fig. 10**). Block T1, monitored by TAS1_1, shows mostly reversible displacement, with both diurnal and annual amplitudes and higher diurnal amplitudes during the warm period of the year. The linear regression between crack-meter position and temperature is low. Block T2, monitored by TAS2_1 and TAS2_2, shows low diurnal and annual amplitudes, with the highest daily amplitudes measured during the spring months. No significant long-term trends were observed, and both crack meters show low linear regression values with temperature. Block T3, monitored by TAS3_1 and TAS3_2, shows relatively high diurnal and annual amplitudes, with the highest diurnal amplitudes measured in autumn. TAS3_1 shows gradual elongation, whereas TAS3_2 shows gradual shortening, representing the highest irreversible trends within the dataset. Block T4, monitored by TAS1_2, shows low annual and diurnal amplitudes, with the highest diurnal amplitudes measured during the summer months. A positive linear relationship between crack-meter position and temperature is present, while no significant long-term trend was recorded.

https://doi.org/10.5194/egusphere-2026-5565
Preprint. Discussion started: 25 September 2026

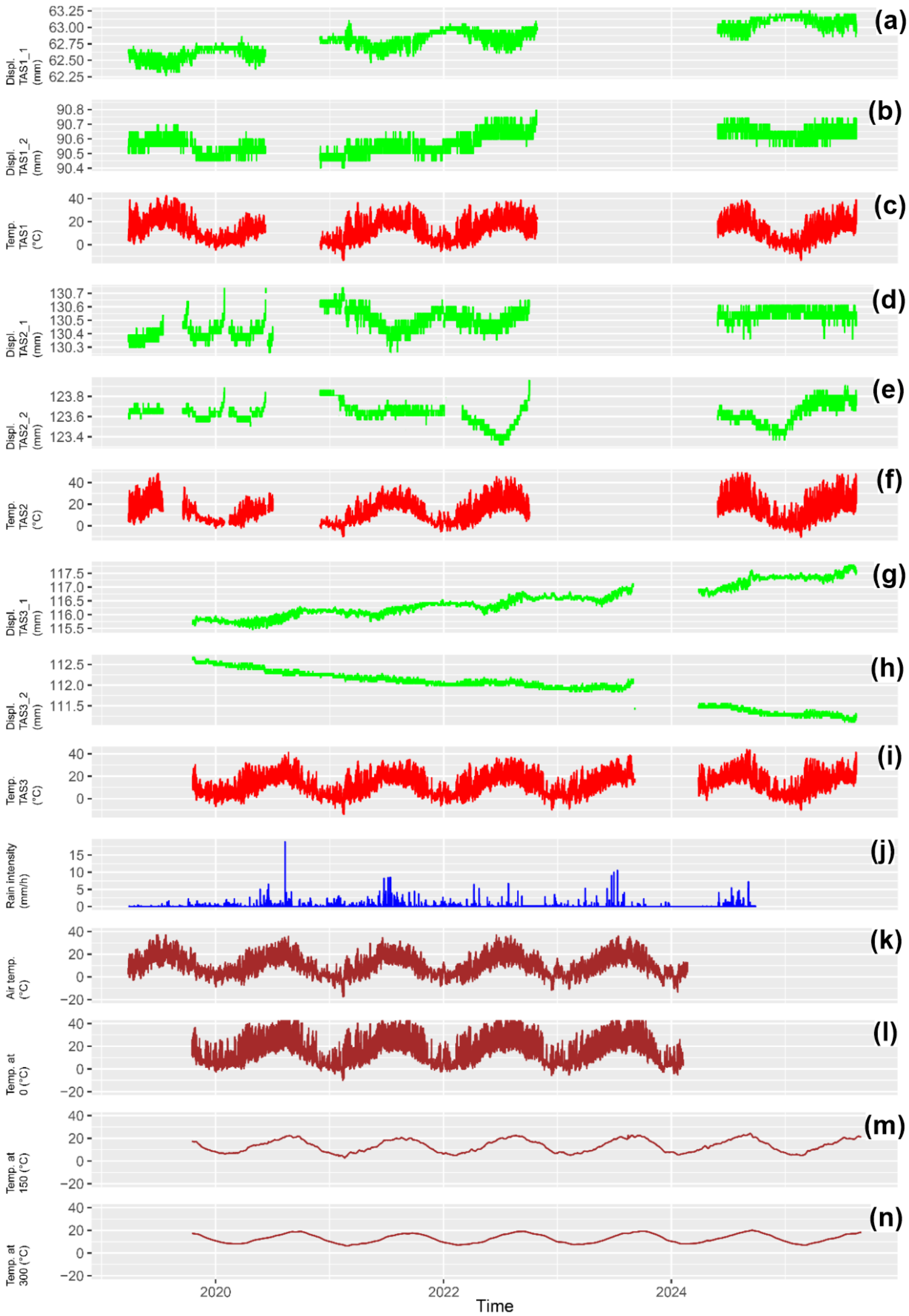

Figure 10. Analysed data from Tašovice between 2020 and 2024, aggregated to 1 h resolution. **(a)** Displacement TAS1_1 (mm); **(b)** Displacement TAS1_2 (mm); **(c)** temperature TAS1 (°C); **(d)** Displacement TAS2_1 (mm); **(e)** Displacement TAS2_2 (mm); **(f)** temperature TAS2 (°C); **(g)** Displacement TAS3_1 (mm); **(h)** Displacement TAS3_2 (mm); **(i)** temperature TAS3 (°C); **(j)** rainfall intensity (mm/h); **(k)** air temperature weather station; **(l)** rock slope surface temperature; **(m)** temperature 150 cm; **(n)** temperature 300 cm.

https://doi.org/10.5194/egusphere-2026-5565
Preprint. Discussion started: 25 September 2026

Statistically significant rainfall-related responses were detected for TAS1_1, TAS3_1, and TAS3_2 (Table 4). TAS1_1 showed a positive response for three rainfall/response-window combinations. For block T3, TAS3_1 showed positive responses for six combinations, whereas TAS3_2 showed negative responses for nine combinations.

3.1.4 Labský důl

Labský důl is the coldest monitored site, with an average annual temperature of 4.59 °C. The long-term stable temperature (LST) reaches 4.8 °C, while the stable temperature depth (STD) is 16.6 m. The site exhibits relatively low daily temperature amplitudes in the near-surface zone, which decrease exponentially with depth.

Labský důl shows variable crack-meter displacement patterns across the four monitored blocks (L1–L4) (**Table 3; Fig. 11**). Block L1, monitored by LAB1_1, shows both annual and diurnal displacement amplitudes, with the highest diurnal amplitudes measured during the spring season. No significant irreversible trend was recorded, while a relatively strong negative relationship between crack-meter position and temperature was observed. Block L2, monitored by LAB1_2, also shows annual and diurnal amplitudes, with the highest diurnal amplitudes during spring, together with a slow closing trend and a weak relationship with temperature. Blocks L3 and L4, monitored by LAB3_1 and LAB3_2, show highly irregular displacement patterns with seasonal dilation and contraction. LAB3_1 shows both diurnal and annual amplitudes and rapid reversible displacement changes, whereas LAB3_2 shows an overall positive displacement trend. A positive relationship between crack-meter position and temperature was also recorded for LAB3_2.

https://doi.org/10.5194/egusphere-2026-5565
Preprint. Discussion started: 25 September 2026

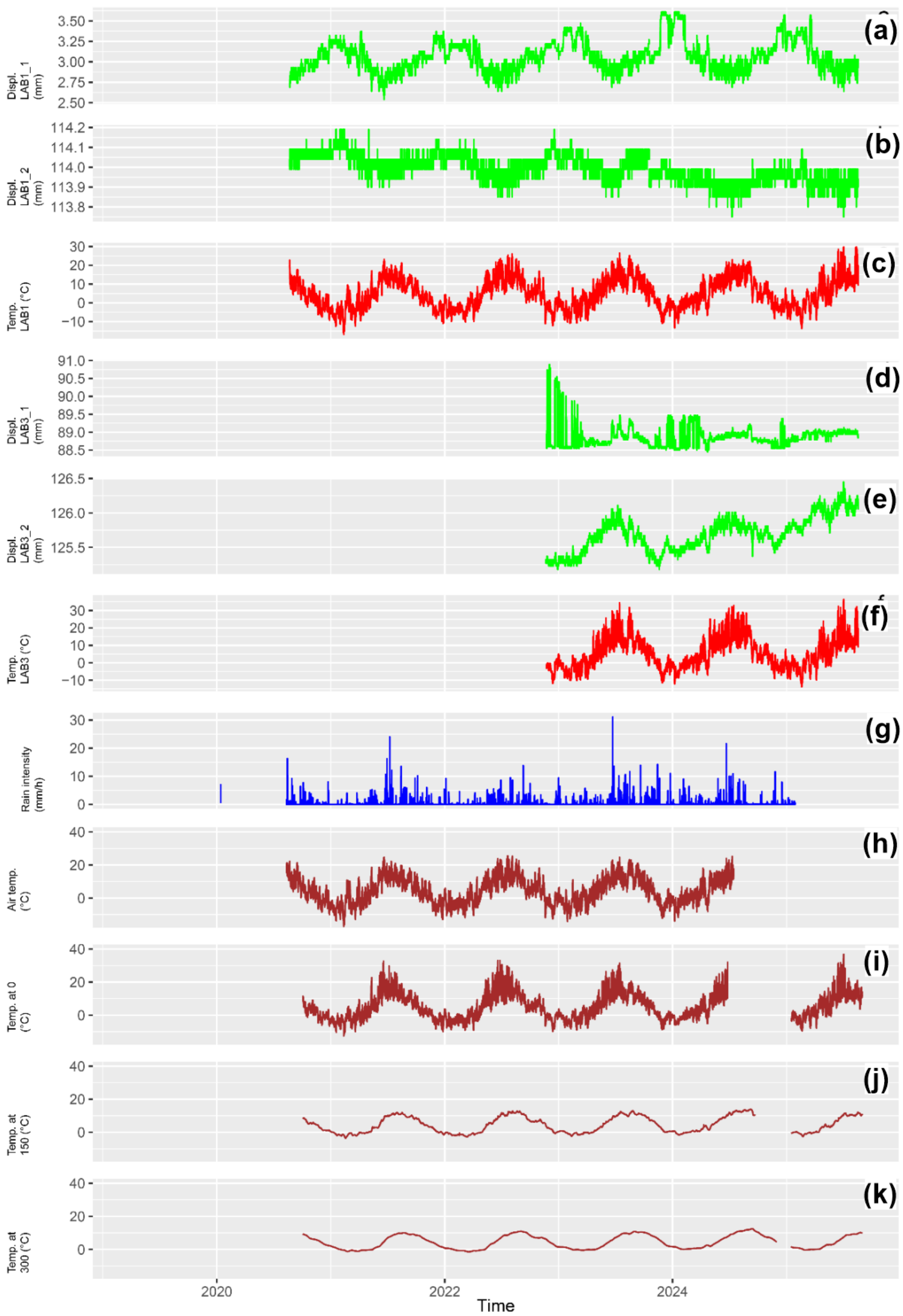

Figure 11. Analysed data from Labský důl aggregated to 1 h resolution. **(a)** Displacement LAB1_1 (mm); **(b)** Displacement LAB1_2 (mm); **(c)** temperature LAB1 (°C); **(d)** Displacement LAB3_1 (mm); **(e)** Displacement LAB3_2 (mm); **(f)** temperature LAB3 (°C); **(g)** rainfall intensity (mm/h); **(h)** air temperature weather station; **(i)** rock slope surface temperature; **(j)** temperature 150 cm; **(k)** temperature 300 cm.

Statistically significant rainfall-related responses were detected for LAB3_1 and LAB3_2 (Table 4). LAB3_1 showed a significant response for only one rainfall/response-window combination, whereas LAB3_2 showed significant responses for four combinations. No significant rainfall-related responses were detected for LAB1_1 and LAB1_2.

3.2 Meteorologically induced crack meter dynamics

To identify common patterns across the monitoring sites, the relationships between crack-meter displacement and meteorological forcing were evaluated across the complete dataset. The following sections separately summarize temperature-related displacement dynamics and crack-meter responses to extreme rainfall events, including their relationship with long-term irreversible displacement trends (**Tables 3 and 4; Fig. 12**).

3.2.1 Temperature

Both diurnal and annual displacement cycles are present across the monitored crack meters, although their magnitude and temporal behaviour vary considerably between individual sensors (Table 3). Annual amplitudes range from low values recorded for several sensors at Branická Rock, Tašovice and Labský důl to amplitudes exceeding 1 mm at Pastýřská Rock and for block T3 at Tašovice. Diurnal displacement amplitudes also vary among sensors, and their seasonal maxima occur at different times of the year. Spring maxima are common for several sensors at Branická Rock and Labský důl, while summer maxima are recorded for TAS1_1 and TAS1_2 and autumn maxima for PAS2_1, PAS2_2, BRA3_1, BRA3_2, TAS3_1, TAS3_2 and LAB3_2 (Table 3).

The relationship between crack-meter position and temperature varies substantially across the dataset (Table 3; **Fig. 12**). Negative relationships predominate, with all four crack meters at Pastýřská Rock showing consistent negative linear regression coefficients between position and temperature. Negative relationships are also recorded for several crack meters at Branická Rock and Labský důl. In contrast, positive relationships are less frequent and are most clearly represented by TAS1_2 at Tašovice and LAB3_2 at Labský důl. Several other sensors, particularly at Branická Rock and Tašovice, show relatively low linear regression coefficients, indicating only a weak linear relationship between crack-meter position and temperature (Table 3).

Pearson correlation analysis further shows that crack-meter displacement is generally more strongly related to air and near-surface rock temperatures than to temperatures measured deeper within the rock mass (**Fig. 12**). Correlations generally decrease for temperature records at depths of 150 and 300 cm, and no systematic increase in correlation with deeper rock temperature was observed across the monitoring sites. The strength and direction of these correlations nevertheless vary between individual crack meters.

Temperature relationships also differ according to the presence of long-term displacement trends (Table 3; **Fig. 12**). Crack meters with strong negative temperature relationships generally show low or no irreversible displacement trends. In contrast, several sensors with relatively weak temperature relationships show pronounced long-term opening or closing trends. This is particularly evident for BRA1_1 and BRA1_2 at Branická Rock and TAS3_1 and TAS3_2 at Tašovice. TAS3_1 records the strongest positive displacement trend within the dataset, whereas TAS3_2 records the strongest negative trend. LAB3_2 differs from this general pattern by combining a positive relationship with temperature with a pronounced positive long-term displacement trend.

https://doi.org/10.5194/egusphere-2026-5565
Preprint. Discussion started: 25 September 2026

Table 3. Results of crack meter measurements across all four monitoring sites. YA: average annual amplitude, DA: average diurnal amplitude, DAmax: maximal measured diurnal amplitude, DAm: month of maximal measured diurnal amplitude, LR pos/T: linear regression coefficient between crack meter position and temperature, trend: irreversible trend of crack meter displacement.

Site	Block	Crack meter	YA [mm]	DA [mm]	DAmax [mm]	DAm [month]	LR pos/T	Trend [mm yr^{-1}]
Pastýřská Rock	P1	PAS1_1	0.71	0.034	0.128	April	-0.012	-0.077
		PAS1_2	0.78	0.037	0.139	April	-0.015	-0.134
		PAS2_1	1.12	0.051	0.171	October	-0.0199	-0.062
		PAS2_2	0.97	0.047	0.163	October	-0.015	-0.077
Branická Rock	B1	BRA1_1	0.53	0.028	0.103	March	-0.0019	0.214
		BRA1_2	0.61	0.03	0.108	April	-0.0049	0.103
	B2	BRA2_1	0.48	0.026	0.095	March	-0.0027	-0.007
		BRA2_2	0.56	0.029	0.102	April	-0.00001	-0.033
	B3	BRA3_1	0.64	0.033	0.117	October	-0.0087	-0.01
		BRA3_2	0.7	0.035	0.123	October	-0.0076	-0.041
	B2	BRA4_1	0.5	0.027	0.098	March	-0.0033	-0.074
Tašovice	T1	TAS1_1	0.44	0.023	0.084	July	-0.0041	0.093
	T4	TAS1_2	0.48	0.025	0.089	July	0.0049	0.02
	T2	TAS2_1	0.6	0.032	0.113	April	-0.0023	0.023
		TAS2_2	0.63	0.034	0.119	April	-0.00082	-0.004
	T3	TAS3_1	0.88	0.052	0.176	October	0.004	0.308
		TAS3_2	0.81	0.048	0.167	October	-0.0046	-0.226
Labský důl	L1	LAB1_1	0.55	0.022	0.081	April	-0.019	0.021
	L2	LAB1_2	0.35	0.019	0.069	April	-0.0039	-0.03
	L3	LAB3_1	0.46	0.028	0.102	October	0.011	0.005
	L4	LAB3_2	0.64	0.036	0.129	October	0.019	0.228

3.2.2 Rainfall

Direct correlations between hourly rainfall intensity and crack-meter position were weak across the dataset and did not reveal a systematic relationship between rainfall and crack-meter displacement (**Fig. 12**). The response of crack-meter position residuals to extreme rainfall events varies considerably across the dataset, with statistically significant responses ($p < 0.05$) restricted to a subset of the monitored crack meters (Table 4). At Pastýřská Rock, significant responses were detected for PAS1_2 and PAS2_2, each for only one rainfall/response-window combination. At Branická Rock, the most frequent significant responses were recorded for BRA1_1 and BRA2_2, with three and five significant combinations, respectively, while BRA1_2 showed a significant response for only one combination. The highest number of significant rainfall responses was observed at Tašovice, particularly for block T3. TAS1_1 responded significantly to three rainfall/response-window combinations, TAS3_1 to six combinations, and TAS3_2 to nine combinations (Table 4). At Labský důl, the rainfall response differed between the monitored crack meters. LAB3_1 showed a significant response for only one rainfall/response-window combination, whereas LAB3_2 showed significant responses for four combinations (Table 4). No significant rainfall-related responses were detected for LAB1_1 and LAB1_2. Overall, isolated significant responses were therefore recorded at Pastýřská Rock, while multiple significant rainfall/response-window combinations occurred for individual crack meters at Branická Rock, Tašovice, and Labský důl.

https://doi.org/10.5194/egusphere-2026-5565
Preprint. Discussion started: 25 September 2026

Table 4. Summary of statistically significant crack-meter responses to extreme rainfall events. Significant rainfall/response windows indicate combinations of rainfall accumulation periods (24, 48, 72, and 96 h) and subsequent crack-meter response periods (72, 168, and 240 h) for which a statistically significant response ($p < 0.05$) was detected. The number of significant combinations summarizes the total number of significant rainfall/response-window combinations identified for each crack meter.

Site	Crack meter	Significant rainfall response	Significant rainfall/response windows	No. significant combinations
Pastýřská Rock	PAS1_P1	No	–	0
	PAS1_P2	Yes (<2)	48/240	1
	PAS2_P1	No	–	0
	PAS2_P2	Yes (<2)	48/72	1
Branická Rock	BRA1_P1	Yes	48/72; 48/240; 96/240	3
	BRA1_P2	Yes (<2)	48/72	1
	BRA2_P1	No	–	0
	BRA2_P2	Yes	24/168; 24/240; 48/72; 48/168; 48/240	5
	BRA3_P1	No	–	0
	BRA3_P2	No	–	0
	BRA4_P1	No	–	0
Tašovice	TAS1_P1	Yes	48/168; 96/168; 96/240	3
	TAS1_P2	No	–	0
	TAS2_P1	No	–	0
	TAS2_P2	Yes (<2)	24/72	1
	TAS3_P1	Yes	24/72; 24/168; 48/72; 48/168; 72/168; 96/168	6
	TAS3_P2	Yes	24/72; 24/168; 24/240; 48/72; 48/168; 48/240; 72/168; 72/240; 96/240	9
Labský důl	LAB1_P1	No	–	0
	LAB1_P2	No	–	0
	LAB3_P1	Yes (<2)	96/240	1
	LAB3_P2	Yes	24/72; 48/72; 48/168; 96/240	4

The significant responses differ not only in their frequency among individual crack meters but also in the rainfall accumulation and subsequent response windows in which they occur (Table 4). Significant responses are frequently associated with response windows extending beyond the duration of the rainfall accumulation period, including 168- and 240-h response windows. Consequently, significant changes in crack-meter position residuals are not restricted to the period immediately following the rainfall event but are also detected over longer response periods.

Across the dataset, crack meters with multiple significant rainfall responses frequently differ from those showing strong negative relationships with temperature (Tables 3 and 4; **Fig. 12**). This pattern is particularly evident for BRA1_1, TAS3_1, and TAS3_2, which combine multiple significant rainfall responses with pronounced irreversible displacement trends. In contrast, most crack meters characterized by strong negative temperature relationships and predominantly reversible displacement patterns show few or no significant rainfall responses. Rainfall sensitivity is nevertheless restricted to a subset of the monitored crack meters and varies substantially between individual sensors.

https://doi.org/10.5194/egusphere-2026-5565
Preprint. Discussion started: 25 September 2026

3.3 Cluster analyses

Hierarchical clustering based on temperature and rainfall sensitivity separated the 21 monitored crack meters into four distinct groups (CL1–CL4), following the classification procedure described in Section 2.2.3. CL1 comprises crack meters characterized predominantly by negative relationships with temperature, whereas CL2 represents sensors with positive temperature relationships. CL3 includes crack meters with weak temperature relationships but significant rainfall sensitivity, while CL4 comprises sensors showing weak relationships with both temperature and rainfall. Nine crack meters were classified as CL1, two as CL2, five as CL3, and the remaining five as CL4. The resulting cluster classification, together with the relationships between crack-meter displacement and the monitored environmental variables, is summarized in **Fig. 12.** The clusters also differ in the magnitude and direction of irreversible displacement trends.

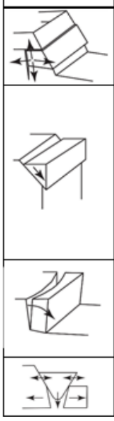

Block geometry with assumed destabilisation direction	Cluster	Crack meter	Volume [m³]	Corr. Temp. Log	Corr. Rain Intensity	Corr. Temp. at 0 cm	Corr. Temp. at 150 cm	Corr. Temp. at 300 cm	Disp. Trend [mm/yr]	p-value rainfall < 0.05 count
	CL1	PAS1_1	150	-0.52	-0.02	-0.51	-0.33	-0.16	-0.077	0
	CL1	PAS1_2	150	-0.45	-0.01	-0.45	-0.32	-0.21	-0.134	1
	CL1	PAS2_1	150	-0.62	-0.01	-0.63	-0.39	-0.17	-0.062	0
	CL1	PAS2_2	150	-0.56	0	-0.56	-0.33	-0.17	-0.077	1
	CL1	BRA2_1	14.9	-0.79	0	-0.84	-0.63	-0.29	-0.007	0
	CL1	BRA3_1	14.4	-0.73	-0.03	-0.68	-0.67	-0.5	-0.01	0
	CL1	BRA3_2	14.4	-0.45	0.07	-0.5	-0.37	-0.21	-0.041	0
	CL1	LAB1_2	0.35	-0.46	0	-0.5	-0.35	-0.23	-0.03	0
	CL3	TAS1_1	2	-0.34	-0.02	-0.14	0.02	0.07	0.093	3
	CL3	BRA2_2	14.9	0.05	0.05	-0.03	0.05	0.12	-0.033	5
	CL4	BRA4_1	14.9	-0.18	0.03	-0.12	-0.01	0.03	-0.074	0
	CL4	TAS2_1	0.3	-0.29	-0.01	-0.27	-0.23	-0.16	0.023	0
	CL4	TAS2_2	0.3	-0.05	0.01	-0.07	-0.17	-0.17	-0.004	1
	CL1	LAB1_1	0.84	-0.81	-0.02	-0.81	-0.62	-0.43	0.021	0
	CL3	BRA1_1	0.5	-0.05	-0.05	-0.03	0.09	0.12	0.214	3
	CL3	TAS3_1	0.25	0.08	-0.05	0.05	0.15	0.15	0.308	6
	CL3	TAS3_2	0.25	-0.1	0.05	-0.08	-0.1	-0.06	-0.226	9
	CL4	BRA1_2	0.5	-0.21	-0.03	-0.21	-0.03	0.08	0.103	1
	CL2	LAB3_2	1.35	0.62	-0.04	0.62	0.45	0.26	0.228	4
	CL2	TAS1_2	2.3	0.61	-0.05	0.64	0.55	0.43	0.02	0
	CL4	LAB3_1	0.84	0.28	0.1	0.25	0.09	0.04	0.005	1

Figure 12. Values of the correlation for the different crack meters and monitored variables. The red colour scale corresponds to negative correlations, indicating dynamic mechanisms with consistent variable behaviour. The blue colour indicates positive correlations. Orange, green, magenta, and grey indicate clusters 1, 2, 3, and 4, respectively. The behaviour of sensors classified as CL4 represents complex crack-meter responses without a clearly resolved dominant meteorological control; therefore, these data are presented with a grey mask.

CL1 represents the largest group and includes PAS1_1, PAS1_2, PAS2_1, PAS2_2, BRA2_1, BRA3_1, BRA3_2, LAB1_1, and LAB1_2. These crack meters are characterized by negative correlations between position and temperature (**Fig. 12**). Both annual and diurnal displacement cycles are present, while long-term irreversible displacement trends are generally low. Rainfall sensitivity is also low, with no systematic response to extreme rainfall events identified for the CL1 sensors. This cluster occurs at Pastýřská Rock, Branická Rock, and Labský důl, but is absent at Tašovice.

CL2 contains only two crack meters, TAS1_2 and LAB3_2, and is distinguished from CL1 by a positive relationship between crack-meter position and temperature. Both sensors show positive correlations with air and rock-surface temperatures (**Fig. 12**). TAS1_2 shows only a minor long-term displacement trend, whereas LAB3_2 exhibits a pronounced positive trend. Thus, despite their similar positive temperature relationships, the magnitude of irreversible displacement differs between the two CL2 sensors.

CL3 comprises BRA1_1, BRA2_2, TAS1_1, TAS3_1, and TAS3_2. In contrast to CL1 and CL2, these crack meters show weak correlations with temperature but systematic responses to extreme rainfall events (**Fig. 12**). The group also contains several of the strongest irreversible displacement trends in the dataset. BRA1_1, TAS1_1, and TAS3_1 show positive long-term trends, whereas TAS3_2 shows a pronounced negative trend. BRA2_2 differs from the other CL3 sensors by showing only a weak negative long-term trend.

The remaining five crack meters are classified as CL4 and show weak relationships with both temperature and rainfall. This group includes BRA1_2, BRA4_1, TAS2_1, TAS2_2, and LAB3_1. Temperature correlations are generally low, and no systematic rainfall response is identified. Most CL4 crack meters also show relatively low

https://doi.org/10.5194/egusphere-2026-5565
Preprint. Discussion started: 25 September 2026

long-term displacement trends, although BRA1_2 exhibits a more pronounced positive trend. CL4 sensors occur at Branická Rock, Tašovice, and Labský důl.

4 Discussion

The observed crack-meter dynamics reflect the interaction between meteorological forcing and the structural and geometrical configuration of individual rock-slope features. The following discussion therefore evaluates the effects of temperature and rainfall, the role of block geometry and kinematic setting, and the resulting thermo-mechanical regimes identified by cluster analysis. Finally, the main limitations and implications for rock-slope monitoring are discussed.

4.1 Meteorological controls on crack meter dynamics

Meteorological forcing is reflected in the crack-meter displacement records through both temperature-related cycles and responses to extreme rainfall events. However, the magnitude, direction, and temporal characteristics of these responses vary considerably among individual monitored features. The effects of temperature and rainfall are therefore discussed separately in the following sections.

4.1.1 Temperature

The monitored crack-meter time series demonstrate that temperature variations are closely linked with joint displacement dynamics across all four sites, although the magnitude and direction of the response differ between individual sensors (**Fig. 12**). The predominantly negative relationships between crack-meter position and air or rock-surface temperature are consistent with thermally induced volumetric changes of the monitored rock mass. This behaviour is particularly clear at Pastýřská Rock, where all four crack meters show similar reversible displacement patterns and only minor long-term closing trends. The observed joint closing tendency may reflect slow rock-mass relaxation in combination with long-term temperature changes during the monitoring period. Similar reversible temperature-related displacement was also recorded for several crack meters at Branická Rock and Labský důl. Such short- and medium-term thermally induced joint displacement has been widely documented in previous studies (Bakun-Mazor et al., 2013; Collins and Stock, 2016; Gasc-Barbier et al., 2021; Merrien-Soukatchoff and Gasc-Barbier, 2023).

The stronger relationships of crack-meter displacement with air and rock-surface temperatures than with temperatures measured at greater depth indicate that the observed thermal response is primarily associated with temperature changes within the shallow rock-slope zone (**Fig. 12**). This is consistent with the rapid attenuation of diurnal temperature amplitudes with depth observed at all monitoring sites. Surface thermal conditions are additionally affected by slope aspect and direct solar radiation, as indicated by the higher near-surface temperature amplitudes at the south-exposed Branická Rock and Tašovice sites. The timing of maximum diurnal crack-meter amplitudes also differs between monitored blocks, ranging from spring maxima at several Branická Rock and Labský důl sensors to summer or autumn maxima at Tašovice and Pastýřská Rock. These differences indicate that the response of individual monitored features to thermal forcing is not uniform.

In two cases, TAS1_2 and LAB3_2, the relationship with temperature is positive rather than negative (**Fig. 12**), demonstrating that thermal forcing can also produce displacement patterns opposite to those expected from simple rock-mass contraction and expansion. A similar effect of temperature was previously observed by Bakun-Mazor et al. (2013) and Guerin et al. (2021). This distinction is also reflected in the cluster analysis, where crack meters characterized predominantly by negative and positive temperature relationships are separated into CL1 and CL2, respectively. The occurrence of different temperature-related displacement patterns indicates that the measured response is modified by the geometry and kinematic configuration of individual monitored features. These geometrical and kinematic controls are discussed further in Section 4.2, while the resulting cluster classification is evaluated in Section 4.3.

4.1.2 Rainfall

In contrast to temperature, the influence of rainfall on crack-meter displacement is not clearly expressed by the direct correlation analysis (**Fig. 12**). A simple correlation between rainfall and crack-meter position does not account for the potentially delayed response of the rock mass to precipitation. The additional event-response analysis, in which different rainfall accumulation and subsequent displacement-response windows were evaluated, revealed statistically significant rainfall-related responses for a subset of the monitored crack meters (Table 4).

This approach therefore identified rainfall-related displacement patterns that were not evident from the direct correlations alone.

The rainfall-related response varies considerably among sites and individual sensors. The most pronounced responses are recorded for BRA1_1, BRA2_2, TAS3_1, TAS3_2 and LAB3_2, whereas the predominantly reversible crack meters at Pastýřská Rock show only isolated significant responses (Table 4). Several rainfall-sensitive crack meters also exhibit irreversible opening or closing trends, particularly BRA1_1 and TAS3_1/TAS3_2. Significant responses are commonly associated with longer response windows rather than only with the period immediately following rainfall, indicating that rainfall-related displacement may develop over several days. Similar medium-term effects of precipitation on rock-slope kinematics and rockfall activity have been reported by Krautblatter and Moser (2009), Wei et al. (2014) and Leinauer et al. (2024).

The delayed rainfall response may reflect several processes related to water infiltration into the rock mass and discontinuities, including increasing groundwater levels, progressive rock-mass saturation, and changes in pore pressure within joints. Similar mechanisms have been described by Hugentobler et al. (2022) and Oestreicher et al. (2023) at the rock-slope scale. These processes may require time to develop after the onset of precipitation and can therefore produce displacement responses extending beyond the duration of the rainfall event itself. However, the present monitoring does not directly measure groundwater conditions or pore pressure, and these mechanisms therefore remain possible explanations rather than directly observed processes. The occurrence of both positive and negative crack-meter responses further indicates that rainfall-related deformation depends on the displacement direction recorded by the individual sensor and the kinematic behaviour of the monitored block.

Overall, both temperature variations and extreme rainfall events are associated with measurable changes in crack-meter displacement, but their expression varies substantially among individual monitored features. Temperature-related displacement is widespread across the dataset and is commonly expressed as reversible diurnal and annual cycles, whereas systematic rainfall responses occur only for a subset of crack meters and are frequently associated with longer response windows and irreversible displacement trends. The absence of a uniform meteorological response across sensors exposed to comparable environmental conditions indicates that meteorological forcing alone cannot explain the observed displacement patterns. The influence of block geometry and kinematic setting on the measured response is therefore considered in the following section.

4.2 Block geometry and kinematic setting

The substantial variability in crack-meter displacement magnitude and temporal behaviour indicates that the response to meteorological forcing is strongly modified by the geometry and kinematic setting of individual monitored rock-slope features (Cifeca Recinella et al., 2026; Gischig et al., 2011). The strength and direction of the relationship between temperature and crack-meter position vary among sensors, as do irreversible displacement trends and sensitivity to rainfall (**Fig. 12**). These differences occur not only between sites but also between neighbouring blocks exposed to similar meteorological conditions. This indicates the influence of individual block geometry, volume, kinematic regime, and the orientation of the monitored discontinuity on the measured displacement response.

The simplest behaviour is observed where crack meters monitor relatively stable blocks and the measured displacement predominantly reflects thermally induced volumetric changes. Pastýřská Rock provides the clearest example, where all four crack meters installed on the same large block show similar reversible displacement patterns and negative relationships with temperature. Comparable behaviour is observed for several blocks at Branická Rock and Labský důl (**Fig. 12**). In these configurations, expansion of the monitored rock mass during warm periods results in joint closure, whereas cooling produces joint opening. The absence of pronounced irreversible displacement indicates that these cyclic movements do not necessarily represent progressive destabilization, despite relatively large annual and diurnal displacement amplitudes. Similar large-amplitude cyclic joint movements driven predominantly by seasonal and diurnal temperature variations have been observed in other monitored rock slopes (Bakun-Mazor et al., 2013; Weber et al., 2017).

More complex geometrical configurations can substantially modify this simple relationship. Only two crack meters, TAS1_2 and LAB3_2, show a clear positive relationship with temperature (**Fig. 12**). At Tašovice, TAS1_2 monitors the weathered wedge-shaped block T4. Its positive temperature relationship can be explained by interaction with the surrounding rock mass, where thermal expansion of neighbouring blocks during warm periods may push the wedge-shaped block upwards and consequently elongate the crack meter. A similar but more pronounced configuration occurs at Labský důl, where blocks L3 and L4 form a wedge-ratchet system. Expansion

https://doi.org/10.5194/egusphere-2026-5565
Preprint. Discussion started: 25 September 2026

of both the monitored block and the wedging block L3 can produce increasing displacement measured by LAB3_2 during warm periods. Such wedging-ratcheting configurations have previously been described as geometrical settings in which thermal expansion of neighbouring rock blocks can generate progressive displacement (Bakun-Mazor et al., 2020; Pasten et al., 2015). The thermally induced strain field can therefore be strongly modified by the geometry of a specific block and its interaction with the surrounding rock mass (Bakun-Mazor, 2022).

Kinematic setting is also important for blocks undergoing gravitationally driven displacement. At Branická Rock, block B1 represents a toppling configuration, with progressive opening measured by BRA1_1 and BRA1_2 superimposed on cyclic displacement. At Tašovice, the opposite long-term trends recorded by TAS3_1 and TAS3_2 on the same toppling block T3 provide another example of how the measured displacement depends on sensor position relative to block movement. Elongation of the upper crack meter and shortening of the lower crack meter represent different components of the same block-scale kinematic process rather than contradictory deformation patterns. Both blocks also show rainfall-related responses, demonstrating that meteorological forcing can be superimposed on ongoing gravitational displacement rather than producing a uniform displacement signal. The importance of geometrical constraints is also illustrated by blocks for which the expected destabilization mode is not clearly reflected in the crack-meter time series. Branická block B2 is structurally predisposed to sliding along an inclined bedding plane, yet BRA2_1 and BRA2_2 show no pronounced long-term opening trend. The mechanical support provided by the stable rock mass at the base of the block may constrain displacement in the expected sliding direction. Similarly, some small and geometrically complex blocks at Tašovice and Labský důl show weak or irregular relationships with the monitored meteorological variables despite being located in potentially unstable configurations. In such cases, interactions with neighbouring blocks can modify the local strain field and the displacement component recorded by an individual crack meter. Such geometrical controls have also been demonstrated by thermo-mechanical modelling and field monitoring by Cifeca Recinella et al. (2026) or Morcioni et al. (2022).

Block volume may represent an additional control, although its influence cannot be isolated from geometry and kinematic setting in the present dataset. The monitored features differ substantially in size and shape, and directly comparable blocks are not available across the four lithological and climatic settings. No systematic differences in crack-meter behaviour attributable to lithology were identified. Differences in the coefficient of thermal expansion between rock types may be relatively small (Waples and Waples, 2004) and, at the scale of the monitored features, may be overshadowed by differences in block geometry and kinematic configuration. Therefore, the similarity of displacement patterns between sites should not be interpreted as evidence that lithology has no influence, but rather that its effect cannot be separated from the substantial geometrical variability of the monitored blocks in the present dataset.

Overall, the observations demonstrate that block geometry and kinematic setting strongly control how meteorological forcing is translated into the displacement recorded by individual crack meters. Reversible negative temperature relationships, positive temperature responses associated with interacting blocks, irreversible toppling-related trends, and more complex displacement patterns can occur under comparable meteorological forcing depending on the configuration of the monitored feature. The resulting variability is reflected in the four groups identified by the cluster analysis (**Fig. 12**), which integrates temperature and rainfall sensitivity with the observed displacement behaviour and is discussed in the following section.

4.3 Cluster analyses and TM regimes

The cluster analysis integrates the variability in temperature and rainfall sensitivity described above and provides a framework for comparing crack-meter dynamics across different sites and kinematic settings (**Fig. 12**). Rather than representing individual monitoring sites or lithologies, the four resulting clusters reflect different combinations of meteorological response, block geometry, kinematic configuration, and monitoring setup. Individual clusters occur across multiple sites, indicating that similar displacement regimes can develop under different climatic and lithological conditions when the monitored blocks have comparable dynamic characteristics.

Cluster **CL1** represents the most consistent temperature-related displacement regime. Crack meters within this group show negative relationships between position and temperature and typically record reversible joint deformation, with both diurnal and annual displacement cycles, caused by rock mass volumetric changes. Irreversible displacement trends are generally low, and no systematic rainfall response is observed. CL1 includes crack meters from Pastýřská Rock, Branická Rock, and Labský důl, supporting the observation that this type of displacement is not restricted to a particular lithology or climatic setting. In the present dataset, CL1 therefore

https://doi.org/10.5194/egusphere-2026-5565
Preprint. Discussion started: 25 September 2026

represents predominantly stable blocks for which cyclic thermal deformation constitutes the main component of the measured joint displacement.

Cluster **CL2** represents a distinctly different thermal response. Only TAS1_2 and LAB3_2 belong to this group, and both show a positive relationship between crack-meter position and temperature (**Fig. 12**). As discussed in Section 4.2, this behaviour is associated with specific block geometries in which thermal expansion of neighbouring rock blocks modifies the local strain field and produces displacement in the opposite direction to that expected from simple joint closure during warming. CL2 therefore demonstrates that a positive temperature relationship does not imply an absence of thermal control, but rather a different geometrical translation of thermal expansion into the displacement recorded by the sensor. In the present dataset, this behaviour is associated with wedging-ratcheting configurations.

Cluster **CL3** differs from the temperature-related CL1 and CL2 regimes by combining weak relationships with temperature with systematic responses to extreme rainfall events (**Fig. 12; Table 4**). The group includes BRA1_1, BRA2_2, TAS1_1, TAS3_1, and TAS3_2 and contains several crack meters with pronounced irreversible displacement trends. In particular, BRA1_1 and TAS3_1/TAS3_2 monitor blocks undergoing toppling-related displacement. Their cyclic thermal signal is less pronounced than for CL1 sensors, while the event-response analysis reveals displacement associated with extreme rainfall events. The occurrence of CL3 at both Branická Rock and Tašovice indicates that this response is not site-specific but occurs in different structural settings where ongoing block displacement is present. Importantly, CL3 should not be interpreted as demonstrating that rainfall is necessarily subordinate to gravitational or thermal forcing. Rather, CL3 identifies a regime in which rainfall sensitivity occurs together with progressive displacement. Whether individual rainfall events act as preparatory processes, accelerators of ongoing movement, or potentially contribute to final triggering cannot be distinguished from the present monitoring data.

Cluster **CL4** comprises crack meters showing weak relationships with both temperature and rainfall (**Fig. 12**). Most CL4 sensors monitor relatively small or geometrically complex blocks, for which interactions with neighbouring rock-slope elements may modify the local strain field. CL4 should therefore be regarded as a complex-response group for which no clear meteorological control could be resolved from the available crack-meter data, rather than as evidence for the absence of environmentally driven deformation.

The distribution of clusters among the four monitoring sites further demonstrates the importance of local block-scale conditions. Pastýřská Rock is represented entirely by CL1 and therefore shows the most homogeneous displacement regime, consistent with the four crack meters monitoring the same large and relatively stable block. Branická Rock contains CL1, CL3, and CL4 sensors, reflecting the contrasting behaviour of its stable, sliding, and toppling blocks. Tašovice contains CL2, CL3, and CL4 and lacks CL1, consistent with the greater geometrical complexity and variability of the monitored features at this site. Labský důl contains CL1, CL2, and CL4, including both negatively temperature-related blocks and the positive temperature response associated with the L3–L4 wedge-ratchet configuration. Thus, cluster membership does not follow monitoring site alone but varies according to the characteristics of individual monitored features.

Overall, the cluster analysis provides a useful synthesis of the different crack-meter displacement regimes observed across the dataset. The occurrence of different clusters within individual monitoring sites, together with similar clusters across different lithological and climatic settings, supports the interpretation that block geometry, kinematic configuration, and monitoring setup strongly influence how meteorological forcing is expressed in crack-meter displacement records. At the same time, the classification is based on the environmental variables and monitoring configuration available in this study and should therefore be considered in the context of the methodological limitations discussed in Section 4.4.

4.4 Limitations and implications for rock-slope monitoring

Occasional gaps in the monitoring time series occurred due to sensor malfunction or battery discharge. Despite these interruptions, the multi-year records provided sufficient temporal coverage for the statistical analyses applied in this study.

The interpretation of crack-meter displacement is inherently influenced by the monitoring configuration. Crack meters record displacement only along a single measurement axis, whereas the actual movement of a rock block may be three-dimensional and can deviate from the direction expected during the monitoring design phase. This limitation is particularly important for structurally complex blocks, where interaction with neighbouring rock-slope elements modifies the local strain field. Consequently, the magnitude of irreversible displacement and the strength of relationships with environmental variables depend partly on sensor orientation relative to the actual movement direction. The comparison between neighbouring crack meters monitoring the same block, such as BRA1_1 and BRA1_2, illustrates that different sensor orientations may capture different components of the same block-scale deformation. The slow shortening recorded by LAB1_2 may similarly be influenced by sensor orientation relative to the actual movement of the block.

The structural and geometrical complexity of the monitored features also limits direct comparison between sites. The investigated blocks differ considerably in volume, shape, discontinuity configuration, and expected kinematic setting. Because directly comparable blocks are not available across the four sites, the effects of individual controls such as lithology, block volume, or climatic setting cannot be isolated independently.

The monitored environmental variables represent another limitation. Temperature was measured in detail both at the surface and within the rock mass, whereas the hydrological processes potentially associated with rainfall-related displacement were not directly monitored. Groundwater level, water content, joint-water pressure, and pore-pressure changes were not measured, and the mechanisms proposed for the delayed rainfall response therefore remain interpretative. Additional hydrological monitoring would be required to distinguish between possible infiltration-related processes and to determine how they contribute to the observed crack-meter response. Similarly, at Labský důl, snow accumulation, ice formation, frost action, and wind may contribute to the highly variable displacement of individual blocks, but these variables are not directly represented in the present dataset.

The hierarchical clustering provides a useful framework for comparing crack-meter behaviour, but the resulting regimes should therefore not be considered universal classifications of rock-slope dynamics. The clusters are based on the environmental variables, statistical thresholds, and sensor configurations available in this study, and unresolved responses may reflect environmental forcing not included in the analysis or limitations of the monitoring configuration. Cluster assignment should therefore be interpreted together with field observations of block geometry and kinematic setting rather than independently from the structural context.

Despite these limitations, the results demonstrate the value of combining long-term crack-meter monitoring with detailed temperature measurements, rainfall analysis, and structural characterization of individual rock-slope features. Monitoring design should consider not only the expected direction of destabilization but also possible interactions between neighbouring blocks and the potential for the displacement direction to evolve over time. Where complex movement is expected, multiple sensors with different orientations or three-dimensional displacement monitoring may provide a more complete representation of block dynamics than a single crack meter.

The results also highlight the importance of separating reversible meteorologically related deformation from irreversible displacement trends when interpreting rock-slope monitoring data. Large diurnal or annual displacement amplitudes do not necessarily indicate progressive destabilization, while relatively small cyclic signals may occur together with pronounced long-term trends. Likewise, the absence of a strong direct correlation with rainfall does not exclude rainfall-related displacement when the response is delayed. Combining long-term trends, temperature relationships, event-response rainfall analysis, and field-based kinematic interpretation therefore provides a more robust basis for evaluating the state and evolution of monitored rock-slope features.

Overall, the monitoring strategy should be adapted to the geometry and expected kinematics of the investigated feature rather than relying on a uniform sensor configuration.

5 Conclusions

This study presents a multi-year monitoring dataset from four sites in Czechia. Within these sites, twenty-one monitoring points were established. The dataset represents diverse lithological, morphological, geometrical, and kinematic settings. The multi-site monitoring approach allowed us to compare how different partial rock slope features respond to thermal and precipitation forcing.

The results demonstrate that temperature cycles and connected thermal expansion of the rock mass represent a dominant driver of joint short-term reversible dynamics across all sites. However, the magnitude, symmetry, and reversibility of these displacements vary significantly depending on monitored block geometry and kinematic regime, and they vary considerably between sites and individual monitoring points. A systematic response to extreme rainfall events was detected only for a subset of crack meters, predominantly monitoring blocks

https://doi.org/10.5194/egusphere-2026-5565
Preprint. Discussion started: 25 September 2026

undergoing ongoing destabilisation. In contrast, no systematic rainfall effect was observed for stable blocks dominated by reversible thermally induced dynamics.

To address this variability, hierarchical clustering analysis revealed three characteristic crack meter regimes, while the last cluster comprises crack meters with complex responses, including sensors with suboptimal installation geometry. These regimes reflect the interaction between joint dynamics and meteorological forcing. Stable, larger blocks are mainly controlled by the thermally driven volumetric changes, while smaller, more complex unstable features are in the combined regime in which both temperature and rainfall affect the joint dynamics. In specific cases (wedging-ratcheting), thermal cycles can also lead to progressive irreversible joint opening, while rainfall-related responses may further accelerate the ongoing gravitationally driven destabilization.

The observations also indicate that the geometry of the monitored feature and the monitoring configuration have stronger control on the observed joint dynamics than lithology or local climatic conditions. The specific geometry of the monitored feature can modify the temperature-induced strain field and produce displacement patterns that differ significantly from the expected gravitationally driven kinematics. The analyses of in-depth temperatures showed a lower influence on the joint dynamics. This indicates that the shallow temperature cycles play the main role in the thermally induced surficial rock slope dynamics.

These results suggest that the thermal cycles are important in the temporal rock slope evolution within the surficial zone up to 3 m deep. Thermally driven deformation, together with other external forcing, can lead to progressive rock slope destabilization, even in the relatively short time frame of several years. The effects of temperature and rainfall modify the destabilization regime, which is defined by the specific geometry of the monitored feature. This is crucial when designing monitoring systems, where it is important to place sensors according to the expected destabilization direction, which can be specifically modified by a specific rock slope geometry. Temperature and rainfall act as preparatory factors in rock slope destabilization, with their effects strongly modified by the geometry of the unstable feature. Under extreme conditions, these factors may also act as triggers; however, such triggering was not captured during the monitoring period.

Importantly, the combination of long-term monitoring and statistical analyses allowed us to identify not only short-term responses to meteorological forcing but also subtle, long-term displacement trends indicative of ongoing block destabilization. These findings underline the importance of thermally induced rock slope dynamics in both temperate and cold climates and suggest that progressive warming may influence slope evolution within ongoing climate change (Racek et al., 2025).

The presented multi-site monitoring demonstrates that meteorological processes acting at the scale of individual rock blocks are an important component of rock slope evolution. Temperature controls short- to medium-term joint dynamics across a wide range of monitored settings, whereas significant rainfall-related responses were observed in blocks exhibiting irreversible displacement trends. These processes and their interaction with block geometry and kinematics should therefore be considered in future studies of rock slope stability.

Data availability

The raw monitoring data underlying this study are publicly available from Zenodo at https://doi.org/10.5281/zenodo.22743669.

Author contribution

OR was responsible for monitoring design and maintenance, study design, data analysis, figure preparation, and writing. ML contributed to data analysis, writing, and figure preparation. **FH** contributed to monitoring design and conceptual supervision. **JB** contributed to monitoring design and maintenance, data collection, data interpretation, and manuscript revision.

Competing interests

The authors declare that they have no conflict of interest.

Acknowledgements

The authors thank the staff of the Institute of Rock Structure and Mechanics of the Czech Academy of Sciences for technical support during field monitoring and maintenance of the monitoring systems. During the preparation

of this manuscript, the authors used ChatGPT to improve the language and grammar. The authors subsequently reviewed and edited the content and take full responsibility for the final manuscript.

Financial support

This research was supported by the Czech Science Foundation (project no. 25-17664S), the Johannes Amos Comenius Programme (P JAC), project no. CZ.02.01.01/00/22_008/0004605, Natural and Anthropogenic Georisks, and by the long-term conceptual development of the research organisation RVO: 67985891.

References

Acharya, A. and Kogure, T.: Application of novel distributed fibre-optic sensing for slope deformation monitoring: a comprehensive review, International Journal of Environmental Science and Technology, 20, 8217–8240, https://doi.org/10.1007/S13762-022-04697-5, 2022.

Araya, S. N., Meding, M., and Berhe, A. A.: Thermal alteration of soil physico-chemical properties: A systematic study to infer response of Sierra Nevada climosequence soils to forest fires, SOIL, 2, 351–366, https://doi.org/10.5194/soil-2-351-2016, 2016.

Bajni, G., Camera, C. A. S., and Apuani, T.: Deciphering meteorological influencing factors for Alpine rockfalls: a case study in Aosta Valley, Landslides, 18, 3279–3298, https://doi.org/10.1007/S10346-021-01697-3, 2021.

Bakun-Mazor, D.: Rock Slope Stability under Temperature Fluctuations, in: Avantgarde Reliability Implications in Civil Engineering, edited by: Hassan, M., IntechOpen, https://doi.org/10.5772/intechopen.108464, 2022.

Bakun-Mazor, D., Hatzor, Y. H., Glaser, S. D., and Santamarina, J. C.: Thermally vs. seismically induced block displacements in Masada rock slopes, Int. J. Rock Mech. Min. Sci., 61, 196–211, https://doi.org/10.1016/j.ijrmms.2013.03.005, 2013.

Bakun-Mazor, D., Keissar, Y., Feldheim, A., Detournay, C., and Hatzor, Y. H.: Thermally-induced wedging–ratcheting failure mechanism in rock slopes, Rock Mech. Rock Eng., 53, 2521–2538, https://doi.org/10.1007/s00603-020-02075-6, 2020.

Bandara, K., Hyndman, R. J., and Bergmeir, C.: MSTL: a seasonal-trend decomposition algorithm for time series with multiple seasonal patterns, International Journal of Operational Research, 52, 79–98, https://doi.org/10.1504/IJOR.2025.143957, 2025.

Blahůt, J. and Racek, O.: Modern Methods of Rock Mass Characterisation and Rockfall Monitoring: A Review, in: Landslides: Detection, Prediction and Monitoring, edited by: Thambidurai, P. and Singh, T. N., Springer, Cham, 1–38, https://doi.org/10.1007/978-3-031-23859-8_1, 2023.

Bottelin, P. and Baillet, L.: Original Insights Into Rock Slope Damage Processes Until Collapse From Passive Seismic Monitoring, Geophys. Res. Lett., 51, e2024GL109139, https://doi.org/10.1029/2024GL109139, 2024.

Bottelin, P., Méric, O., Baillet, L., Beniamine, D., and Lescurier, A.: Mapping rockfall hazard and detecting precursory damage in rock slopes with passive seismic: Lessons from the La Praz case-study, Eng. Geol., 338, 107627, https://doi.org/10.1016/J.ENGGEO.2024.107627, 2024.

Casagli, N., Intrieri, E., Tofani, V., Gigli, G., and Raspini, F.: Landslide detection, monitoring and prediction with remote-sensing techniques, Nature Reviews Earth & Environment, 4, 51–64, https://doi.org/10.1038/s43017-022-00373-x, 2023.

Cifeca Recinella, L., Dattola, G., Rivolta, C., Leva, D., and Crosta, G. B.: Integrated GBInSAR and thermo-mechanical modeling for rock slope displacement analysis across geometrical complexities, Eng. Geol., 369, 108818, https://doi.org/10.1016/J.ENGGEO.2026.108818, 2026.

Cleveland, R. B., Cleveland, W. S., McRae, J. E., and Terpenning, I.: STL: A Seasonal-Trend Decomposition Procedure Based on Loess, J. Off. Stat., 6, 3–73, https://www.scb.se/contentassets/ca21efb41fee47d293bbee5bf7be7fb3/stl-a-seasonal-trend-decomposition-procedure-based-on-loess.pdf, 1990.

https://doi.org/10.5194/egusphere-2026-5565
Preprint. Discussion started: 25 September 2026

Collins, B. D. and Stock, G. M.: Rockfall triggering by cyclic thermal stressing of exfoliation fractures, Nat. Geosci., 9, 395–400, https://doi.org/10.1038/ngeo2686, 2016.

D'Amato, J., Hantz, D., Guerin, A., Jaboyedoff, M., Baillet, L., and Mariscal, A.: Influence of meteorological factors on rockfall occurrence in a middle mountain limestone cliff, Natural Hazards and Earth System Sciences, 16, 719–735, https://doi.org/10.5194/NHESS-16-719-2016, 2016.

D'Angiò, D., Fantini, A., Fiorucci, M., Iannucci, R., Lenti, L., Marmoni, G. M., and Martino, S.: Environmental forcings and micro-seismic monitoring in a rock wall prone to fall during the 2018 Buran winter storm, Natural Hazards, 106, 2599–2617, https://doi.org/10.1007/S11069-021-04556-5, 2021.

Elmouttie, M. and Dean, P.: Systems Engineering Approach to Slope Stability Monitoring in the Digital Mine, Resources, 9, 42, https://doi.org/10.3390/RESOURCES9040042, 2020.

Engel, Z. and Kalvoda, J.: Morphostructural development of the sandstone relief in the Bohemian Cretaceous Basin, https://nomos.is.cuni.cz/publication/33224, last access: 16 January 2026, 2001.

Engel, Z., Nývlt, D., Křížek, M., Treml, V., Jankovská, V., and Lisá, L.: Sedimentary evidence of landscape and climate history since the end of MIS 3 in the Krkonoše Mountains, Czech Republic, Quat. Sci. Rev., 29, 913–927, https://doi.org/10.1016/J.QUASCIREV.2009.12.008, 2010.

Fei, L., Jaboyedoff, M., Derron, M. H., Choanji, T., and Sun, C.: Multiscale observations of diurnal thermal effects on rock failure and crack dynamics in soft marl layers (La Cornalle molasse rock wall, Switzerland), Eng. Geol., 354, 108159, https://doi.org/10.1016/j.enggeo.2025.108159, 2025.

Gage, H. J. M., Nielsen, J. P., and Eyles, C. H.: Temporal variability and site specificity of thermomechanical weathering in a temperate climate, Front. Earth Sci. (Lausanne)., 12, 1318747, https://doi.org/10.3389/FEART.2024.1318747, 2024.

Gariano, S. L. and Guzzetti, F.: Landslides in a changing climate, Earth. Sci. Rev., 162, 227–252, https://doi.org/10.1016/J.EARSCIREV.2016.08.011, 2016.

Gasc-Barbier, M., Merrien-Soukatchoff, V., and Virely, D.: The role of natural thermal cycles on a limestone cliff mechanical behaviour, Eng. Geol., 293, 106293, https://doi.org/10.1016/J.ENGGEO.2021.106293, 2021.

Gasc-Barbier, M., Merrien-Soukatchoff, V., Krzewinski, V., Azemard, P., and Genois, J. L.: Assessment of the influence of natural thermal cycles on dolomitic limestone rock columns: A 10-year monitoring study, Geomorphology, 464, 109353, https://doi.org/10.1016/J.GEOMORPH.2024.109353, 2024.

Gischig, V. S., Moore, J. R., Evans, K. F., Amann, F., and Loew, S.: Thermomechanical forcing of deep rock slope deformation: 1. Conceptual study of a simplified slope, J. Geophys. Res. Earth Surf., 116, F04010, https://doi.org/10.1029/2011JF002006, 2011.

Glawe, U., Zika, P., Zvelebil, J., Moser, M., and Rybar, J.: Time prediction of a rock fall in the Carnic Alps, Quarterly Journal of Engineering Geology, 26, 185–192, https://doi.org/10.1144/GSL.QJEGH.1993.026.003.04, 1993.

Guerin, A., Jaboyedoff, M., Collins, B. D., Stock, G. M., Derron, M.-H., Abellán, A., and Matasci, B.: Remote thermal detection of exfoliation sheet deformation, Landslides, 18, 865–879, https://doi.org/10.1007/s10346-020-01524-1, 2021.

Guillemot, A., Baillet, L., Larose, E., and Bottelin, P.: Changes in resonance frequency of rock columns due to thermoelastic effects on a daily scale: observations, modelling and insights to improve monitoring systems, Geophys. J. Int., 231, 894–906, https://doi.org/10.1093/gji/ggac216, 2022.

Hartmeyer, I. and Otto, J.-C.: Rockfall, glacier recession, and permafrost degradation: long-term monitoring of climate change impacts at the Open-Air-Lab Kitzsteinhorn, Hohe Tauern, DEUQUA Special Publications, 5, 3–12, https://doi.org/10.5194/DEUQUASP-5-3-2024, 2024.

Hugentobler, M., Aaron, J., and Loew, S.: Rock Slope Temperature Evolution and Micrometer-Scale Deformation at a Retreating Glacier Margin, J. Geophys. Res. Earth Surf., 126, e2021JF006195, https://doi.org/10.1029/2021JF006195, 2021.

https://doi.org/10.5194/egusphere-2026-5565
Preprint. Discussion started: 25 September 2026

Hugentobler, M., Aaron, J., Loew, S., and Roques, C.: Hydro-Mechanical Interactions of a Rock Slope With a Retreating Temperate Valley Glacier, J. Geophys. Res. Earth Surf., 127, e2021JF006484, https://doi.org/10.1029/2021JF006484, 2022.

Hungr, O., Evans, S. G., and Hazzard, J.: Magnitude and frequency of rock falls and rock slides along the main transportation corridors of southwestern British Columbia, Can. Geotech. J., 36, 224–238, https://doi.org/10.1139/t98-106, 1999.

Hungr, O., Leroueil, S., and Picarelli, L.: The Varnes classification of landslide types, an update, Landslides, 11, 167–194, https://doi.org/10.1007/S10346-013-0436-Y, 2013.

Janeras, M., Jara, J. A., Royán, M. J., Vilaplana, J. M., Aguasca, A., Fàbregas, X., Gili, J. A., and Buxó, P.: Multi-technique approach to rockfall monitoring in the Montserrat massif (Catalonia, NE Spain), Eng. Geol., 219, 4–20, https://doi.org/10.1016/J.ENGGEO.2016.12.010, 2017.

Janeras, M., Lantada, N., Núñez-Andrés, M. A., Hantz, D., Pedraza, O., Cornejo, R., Guinau, M., García-Sellés, D., Blanco, L., Gili, J. A., and Palau, J.: Rockfall Magnitude-Frequency Relationship Based on Multi-Source Data from Monitoring and Inventory, Remote Sens. (Basel), 15, 1981, https://doi.org/10.3390/rs15081981, 2023.

Krause, D.: Nové poznatky k erozním účinkům a rozsahu pleistocenního ledovce Labského dolu v Krkonoších, Opera Corcontica, 58, 45–58, https://opera.krnap.cz/apex/f?p=103:8:::ANO:8:P8_ROCNIK_ID,P8_CLANEK_ID,P8_CP:58,3,12, 2021.

Krause, D. and Pilous, V.: Geomorfologie Krkonošského národního parku pod drobnohledem, Ochrana přírody, 75, 28–33, https://www.casopis.ochranaprirody.cz/vyzkum-a-dokumentace/geomorfologie-krkonosskeho-narodniho-parku-pod-drobnohledem/, 2020.

Krautblatter, M. and Moser, M.: A nonlinear model coupling rockfall and rainfall intensity based on a four year measurement in a high Alpine rock wall (Reintal, German Alps), Natural Hazards and Earth System Sciences, 9, 1425–1432, https://doi.org/10.5194/nhess-9-1425-2009, 2009.

Larose, E., Carrière, S., Voisin, C., Bottelin, P., Baillet, L., Guéguen, P., Walter, F., Jongmans, D., Guillier, B., Garambois, S., Gimbert, F., and Massey, C.: Environmental seismology: What can we learn on earth surface processes with ambient noise?, J. Appl. Geophys., 116, 62–74, https://doi.org/10.1016/j.jappgeo.2015.02.001, 2015.

Lazar, A., Beguš, T., and Vulić, M.: Monitoring of the Belca rockfall, Acta Geotech. Slov., 15, 2–15, https://doi.org/10.18690/actageotechslov.15.2.2-15.2018, 2018.

Leinauer, J., Dietze, M., Knapp, S., Scandroglio, R., Jokel, M., and Krautblatter, M.: How water, temperature, and seismicity control the preconditioning of massive rock slope failure (Hochvogel), Earth Surface Dynamics, 12, 1027–1048, https://doi.org/10.5194/ESURF-12-1027-2024, 2024.

Liang, F. and Zhen, Z.: Seismic monitoring in rockfall: a literature review, Journal of Engineering Geology, 32, 545–564, https://doi.org/10.13544/j.cnki.jeg.2022-0079, 2024.

Lombardo, L., Cama, M., Maerker, M., and Rotigliano, E.: A test of transferability for landslides susceptibility models under extreme climatic events: application to the Messina 2009 disaster, Natural Hazards, 74, 1951–1989, https://doi.org/10.1007/S11069-014-1285-2, 2014.

Lombardo, L., Fubelli, G., Amato, G., and Bonasera, M.: Presence-only approach to assess landslide triggering-thickness susceptibility: a test for the Mili catchment (north-eastern Sicily, Italy), Natural Hazards, 84, 565–588, https://doi.org/10.1007/S11069-016-2443-5, 2016.

Macciotta, R.: Review and latest insights into rock fall temporal variability associated with weather, Proceedings of the Institution of Civil Engineers - Geotechnical Engineering, 172, 556–568, https://doi.org/10.1680/JGEEN.18.00207, 2019.

Macciotta, R., Martin, C. D., Edwards, T., Cruden, D. M., and Keegan, T.: Quantifying weather conditions for rock fall hazard management, Georisk, 9, 171–186, https://doi.org/10.1080/17499518.2015.1061673, 2015.

https://doi.org/10.5194/egusphere-2026-5565
Preprint. Discussion started: 25 September 2026

MacFarland, T. W. and Yates, J. M.: Introduction to Nonparametric Statistics for the Biological Sciences Using R, Springer, Cham, https://doi.org/10.1007/978-3-319-30634-6, 2016.

Marjanovic, M., Abolmasov, B., Berisavljevic, Z., Pejic, M., and Vranic, P.: Pre-failure deformation monitoring as rockfall prediction tool, IOP Conf. Ser. Earth Environ. Sci., 833, 012197, https://doi.org/10.1088/1755-1315/833/1/012197, 2021.

Marmoni, G. M., Fiorucci, M., Grechi, G., and Martino, S.: Modelling of thermo-mechanical effects in a rock quarry wall induced by near-surface temperature fluctuations, Int. J. Rock Mech. Min. Sci., 134, 104440, https://doi.org/10.1016/j.ijrmms.2020.104440, 2020.

Matsuoka, N.: A multi-method monitoring of timing, magnitude and origin of rockfall activity in the Japanese Alps, Geomorphology, 336, 65–76, https://doi.org/10.1016/J.GEOMORPH.2019.03.023, 2019.

McCarthy, C., Savage, H., and Nettles, M.: Temperature dependence of ice-on-rock friction at realistic glacier conditions, Philos. Trans. A Math. Phys. Eng. Sci., 375, 20150348, https://doi.org/10.1098/RSTA.2015.0348, 2017.

Merrien-Soukatchoff, V. and Gasc-Barbier, M.: The Effect of Natural Thermal Cycles on Rock Outcrops: Knowledge and Prospect, Rock Mech. Rock Eng., 56, 6797–6822, https://doi.org/10.1007/S00603-023-03420-1, 2023.

Morcioni, A., Apuani, T., and Cecinato, F.: The Role of Temperature in the Stress–Strain Evolution of Alpine Rock-Slopes: Thermo-Mechanical Modelling of the Cimaganda Rockslide, Rock Mech. Rock Eng., 55, 2149–2172, https://doi.org/10.1007/s00603-022-02786-y, 2022.

Mulas, M., Marnas, M., Ciccarese, G., and Corsini, A.: Sinusoidal wave fit indexing of irreversible displacements for crackmeters monitoring of rockfall areas: test at Pietra di Bismantova (Northern Apennines, Italy), Landslides, 17, 231–240, https://doi.org/10.1007/S10346-019-01248-X, 2019.

Nava, L., Tordesillas, A., Qian, G., and Catani, F.: Displacement residuals reveal landslide regime shifts, Landslides, 22, 1–16, https://doi.org/10.1007/S10346-024-02353-2, 2024.

Oestreicher, N., Lei, Q., Loew, S., and Roques, C.: Bedrock Fractures Control Groundwater-Driven Mountain Slope Deformations, J. Geophys. Res. Earth Surf., 128, e2022JF006885, https://doi.org/10.1029/2022JF006885, 2023.

Pasten, C., García, M., and Cortes, D. D.: Physical and numerical modelling of the thermally induced wedging mechanism, Géotechnique Letters, 5, 186–190, https://doi.org/10.1680/JGELE.15.00072, 2015.

Pepe, G., Piazza, M., and Cevasco, A.: Geomechanical characterization of a highly heterogeneous flysch rock mass by means of the GSI method, Bulletin of Engineering Geology and the Environment, 74, 465–477, https://doi.org/10.1007/S10064-014-0642-4, 2014.

Priest, S. D. and Hudson, J. A.: Estimation of discontinuity spacing and trace length using scanline surveys, International Journal of Rock Mechanics and Mining Sciences & Geomechanics Abstracts, 18, 183–197, https://doi.org/10.1016/0148-9062(81)90973-6, 1981.

Racek, O. and Blahůt, J.: Rock Mass Characterization and Rockfall Monitoring: Traditional Approaches, in: Landslides: Detection, Prediction and Monitoring, edited by: Thambidurai, P. and Singh, T. N., Springer, Cham, 39–69, https://doi.org/10.1007/978-3-031-23859-8_2, 2023.

Racek, O., Morcioni, A., Blahůt, J., Apuani, T., Štěpánek, P., and Scaringi, G.: Atmospheric warming drives shallow rock slope instability via irreversible joint opening, Landslides, 1–14, https://doi.org/10.1007/S10346-025-02659-9, 2025.

Racek, O., Loche, M., Hartvich, F., and Blahůt, J.: Raw monitoring data for Temperature and Rainfall Effects on Rock Slope Dynamics: Evidence from Multi-Site Monitoring in Czechia, Central Europe, Zenodo [data set], https://doi.org/10.5281/zenodo.22743669, 2026.

https://doi.org/10.5194/egusphere-2026-5565
Preprint. Discussion started: 25 September 2026

Riebe, C. S., Kirchner, J. W., and Finkel, R. C.: Erosional and climatic effects on long-term chemical weathering rates in granitic landscapes spanning diverse climate regimes, Earth Planet. Sci. Lett., 224, 547–562, https://doi.org/10.1016/J.EPSL.2004.05.019, 2004.

Rosser, N., Lim, M., Petley, D., Dunning, S., and Allison, R.: Patterns of precursory rockfall prior to slope failure, J. Geophys. Res. Earth Surf., 112, 4014, https://doi.org/10.1029/2006JF000642, 2007.

Scaringi, G. and Loche, M.: A thermo-hydro-mechanical approach to soil slope stability under climate change, Geomorphology, 401, 108108, https://doi.org/10.1016/j.geomorph.2022.108108, 2022.

Schneider, M., Oestreicher, N., Ehrat, T., and Loew, S.: Rockfall monitoring with a Doppler radar on an active rockslide complex in Brienz/Brinzauls (Switzerland), Natural Hazards and Earth System Sciences, 23, 3337–3354, https://doi.org/10.5194/NHESS-23-3337-2023, 2023.

Sospedra-Alfonso, R., Melton, J. R., and Merryfield, W. J.: Effects of temperature and precipitation on snowpack variability in the Central Rocky Mountains as a function of elevation, Geophys. Res. Lett., 42, 4429–4438, https://doi.org/10.1002/2015GL063898, 2015.

Vařilová, Z., Podroužek, K., Belisová, N., and Horák, J.: Stability deterioration of cliff faces due to historical mining in the Elbe Sandstones Protected Area, Stavební obzor-Civil Engineering Journal, 31, 516–532, https://doi.org/10.14311/CEJ.2022.04.0039, 2022.

Villarraga, C. J., Gasc-Barbier, M., Gendre, V., and Vaunat, J.: The effect of thermal fatigue in a limestone—a laboratory study, in: Landslides and Engineered Slopes. Experience, Theory and Practice, CRC Press, 1987–1993, https://doi.org/10.1201/9781315375007-238, 2018.

Waples, D. W. and Waples, J. S.: A review and evaluation of specific heat capacities of rocks, minerals, and subsurface fluids. Part 1: Minerals and nonporous rocks, Natural Resources Research, 13, 97–122, https://doi.org/10.1023/B:NARR.0000032647.41046.E7, 2004.

Weber, S., Beutel, J., Faillettaz, J., Hasler, A., Krautblatter, M., and Vieli, A.: Quantifying irreversible movement in steep, fractured bedrock permafrost on Matterhorn (CH), Cryosphere, 11, 567–583, https://doi.org/10.5194/TC-11-567-2017, 2017.

Wei, L. W., Chen, H., Lee, C. F., Huang, W. K., Lin, M. L., Chi, C. C., and Lin, H. H.: The mechanism of rockfall disaster: A case study from Badouzih, Keelung, in northern Taiwan, Eng. Geol., 183, 116–126, https://doi.org/10.1016/j.enggeo.2014.10.008, 2014.

Willenberg, H., Spillmann, T., Eberhardt, E., Evans, K., Loew, S., and Maurer, H. R.: Multidisciplinary monitoring of progressive failure processes in brittle rock slopes – Concepts and system design, in: Landslides, Routledge, 477–483, https://doi.org/10.1201/9780203749197-68, 2018.

Zvelebill, J. and Moser, M.: Monitoring based time-prediction of rock falls: Three case-histories, Physics and Chemistry of the Earth, Part B: Hydrology, Oceans and Atmosphere, 26, 159–167, https://doi.org/10.1016/S1464-1909(00)00234-3, 2001.